Spin-charge gauge approach to the pseudogap phase of high-T_c cuprates: Theory versus experiments

P. A. Marchetti

Dipartimento di Fisica "G. Galilei," INFN, I-35131 Padova, Italy

L. De Leo and G. Orso

International School for Advanced Studies (SISSA), INFM, Via Beirut, 34014 Trieste, Italy

Z. B. Su and L. Yu

Institute of Theoretical Physics and Interdisciplinary Center of Theoretical Studies, Chinese Academy of Sciences, 100080 Beijing, China

We consider as a clue to the understanding of the pseudogap phase in high-T_c superconductors the metal-insulator crossover in underdoped, nonsuperconducting cuprates as temperature decreases and a similar crossover in superconducting cuprates when a strong magnetic field suppresses superconductivity. A spin [SU(2)] and charge [U(1)] Chern-Simons gauge field theory, applied to the t-J model, is developed to describe this striking phenomenon. Two length scales have been derived from the theory: the antiferromagnetic correlation length $\xi \approx (\delta|\ln \delta|)^{-1/2}$, where δ is the doping concentration, and the thermal de Broglie wavelength of the dissipative charge carriers $\lambda_T \approx (T\delta/t)^{-1/2}$, where T is the temperature, t the hopping integral. At low temperatures $\xi \lesssim \lambda_T$, the antiferromagnetic short-range order dominates, and the charge carriers become localized, showing insulating behavior. On the contrary, at high temperatures $\xi \gtrsim \lambda_T$, the dissipative motion of charge carriers prevails, exhibiting metallic conductivity. Furthermore, the gauge interaction induces binding of spinons (spin excitation) and holons (charge carrier) into "electron" resonance. This process introduces a new energy scale, the inverse recombination time, which turns out to be essential in the interpretation of the out-of-plane resistivity. The major steps in the theoretical derivation of these results, particularly the calculation of the current-current correlation function and the Green's function for the physical electron, are presented with some detail. The obtained theoretical results are systematically compared with the in-plane and out-of-plane resistivity data and the magnetoresistance data, as well as the nuclear magnetic relaxation data in the pseudogap regime. Very good agreement is obtained.

I. INTRODUCTION

The mechanism of high-T_c superconductivity, a great intellectual challenge posed by Bednorz and Müller to the condensed matter physics community 16 years ago, to a large extent remains unresolved. The understanding of the "pseudogap"—i.e., a suppressed density of states (DOS) near the Fermi level—as one of the most distinctive features of cuprates (particularly in the underdoped regime) from the conventional superconductors, may serve as a key to the high-T_c conundrum. (For a recent review of this issue consult Ref. 1.)

A. Pseudogap phenomenology

A gap in the spin excitation spectrum was first observed in nuclear magnetic resonance (NMR) experiments,[2] showing up as DOS reduction in both Knight shift and spin-lattice relaxation rate, below a certain crossover temperature T^*. Later on, a gap in the charge excitations was also found in transport measurements. Unlike optimally doped cuprates where the linear temperature dependence of the in-plane resistivity extends to very low temperatures, in underdoped samples the temperature dependence becomes sublinear below some characteristic temperature T^* because of the reduced scattering rate due to a gap opening.[3,4] Upon further

decrease of doping a striking metal-insulator crossover (MIC) was observed.[5] The existence of a pseudogap in the normal state of underdoped cuprates was further confirmed by studying the *ab*-plane optical conductivity,[6] specific heat measurements,[7] and many others. However, the most direct evidence of the pseudogap comes from the angle-resolved-photoemission spectroscopy (ARPES) experiments which showed a *d*-wave-like gap in the normal state in Bi-2212 below the crossover temperature T^*.[8] The pseudogap structure in the total density of states was also detected in tunneling experiments on Bi-2212.[9]

The current picture of the pseudogap opening appears as follows:[10] There exists a large Fermi surface (FS) in cuprate superconductors, consistent with predictions of electronic structure studies at high temperatures. As the temperature decreases below T^*, the pseudogap first opens near $(0,\pi)$; it then gradually "eats up" the original FS, converting it into "pseudogapped" part, eventually leaving only short disconnected arcs around $(\pi/2,\pi/2)$. Finally, these arcs shrink to nodal points of the gap function, and the pseudogap converges to the superconducting gap, with the same *d*-wave-like symmetry. Meanwhile, the quasiparticle peak which is ill defined in the normal-pseudogap state, becomes well defined in the superconducting state, like in typical BCS superconductors. This picture seems to be universal for all classes of

cuprate superconductors and is consistent with all available data on pseudogap phenomena.

B. Different schools of thought

However, the smooth crossover of the pseudogap into a superconducting gap does not tell us the *origin* of the pseudogap itself. Theoretical models attempting to interpret the pseudogap are very much diversified, including the nearly antiferromagnetic Fermi (NAFF) liquid approach,[11] the crossover from Bose-Einstein condensation (BEC) to BCS scenario,[12] and many others.[1] Closely related to our approach, there are two schools of thought. According to one school, pseudogap is a "precursor" to superconductivity; i.e., the superconducting state is more fundamental. The other school emphasizes the proximity to the Mott insulating state, considering the pseudogap phase as nothing but doped Mott insulators. Therefore, the normal state is more fundamental, while the superconducting state is derived from this anomalous normal state, as the BCS superconductivity appears when a pairing force is present in the Landau Fermi liquid.

There were several early proposals on the first approach, assuming preformed pairs in the normal state.[13] This approach was developed further by different groups. Emery and Kivelson considered phase fluctuations of the superconducting order parameter which destroy the coherence above T_c.[14] Somewhat related appear the nodal liquid approach[15] and its QED_3 variant.[16] Randeria attempted to derive several properties of the pseudogap phase, starting from a low-density, short-correlation-length superconducting state.[17] It's fair to say that to describe the rich variety of phenomena in the pseudogap phase by superconducting fluctuations alone is a too difficult, if not impossible task.

The other school of thought was pioneered by Anderson.[18] The reference compound before doping is a Mott insulator characterized by a strong on-site Coulomb repulsion. The electrons are basically localized, forming singlet pairs. A finite amount of energy (spin gap) is needed to break this singlet pair. Although similar to superconducting singlet pairing, this state itself is very different from the superconducting state. A mean-field theory using the spin-charge separation concept and "slave boson" technique was developed very early.[19] To implement the single-occupancy constraint coming from the on-site repulsion and to describe the interaction between "slave" particles a gauge field theory was developed.[20,21] First the U(1) gauge field theory,[22] then the SU(2) gauge field theory[23] was developed to account for various properties of the pseudogap phase by Lee and co-workers. The transport properties in the pseudogap phase were also considered using the U(1) gauge field model.[24] A new version of this approach was formulated recently in terms of "spinons," "chargons," and "visons" with some predictions to be verified by experiments.[25]

A different, but related approach is to associate the pseudogap phase with a quantum critical point (QCP).[26] It was proposed that the strong fluctuations near the QCP may be responsible for superconducting pairing and anomalous properties in the normal state.[27] What is the order parameter related to this quantum phase transition? There were several proposals[27,28] to be checked by experiments. By extrapolating the curve $T^*(\delta)$, where δ is the doping concentration to temperatures below T_c, a "critical concentration" $\delta_c \sim 0.19$ was identified, where the superconducting condensation energy also reaches a maximum.[29] The specific heat jump at the superconducting transition changes its doping dependence at this point as well.[29] These authors argue that below the QCP the short-range antiferromagnetic correlations dominate, giving way to superconducting ordering at that point.

Before resorting to a review our own work we would like to mention a recent scanning tunneling microscopy (STM) experiment exhibiting explicitly the competition and coexistence of the pseudogap and superconducting phases.[30] The STM pattern seems to be messy: the superconducting regions are separated by pseudogap areas at nanoscale, but are kept coherent as Josephson arrays. However, these two types of regions refuse to mix with each other, as Zaanen put it pictorially,[31] like "oil and vinegar in salad dressing." Moreover, these two regions behave totally differently: the typical "resonance" states caused by Ni impurities in the superconducting areas disappear completely in the pseudogap phase. This means these two phases, in spite of their apparent similarity, are of different nature.[32] To elucidate their competition and coexistence is a real challenge to theory.

C. Clue to the problem

What is the key to the understanding of the pseudogap phase? An "obvious" answer is the pseudogap formation— i.e., to explain how a gap is originated and how the states are filled in as the temperature increases. Apparently this is not enough, as we know that one scale or a single variable usually cannot give rise to a "show" in physics. There must be some competition. Our attention was attracted by the spectacular MIC observed in underdoped, nonsuperconducting cuprates in the absence of a magnetic field and a similar phenomenon in superconducting samples when an applied strong magnetic field suppresses the superconductivity.

First of all, this crossover is a rather universal phenomenon. A minimum in resistance (around 50–100 K) and a crossover from metallic conductivity at high temperatures to insulating behavior at low temperatures has been observed in heavily underdoped $La_{2-x}Sr_xCuO_4$ (LSCO) (Refs. 5 and 33), nonsuperconducting $Bi_{2+x}Sr_{2-y}CuO_{6\pm\delta}$ (Ref. 34), and non-superconducting $YBa_2Cu_3O_{7-\delta}$ (YBCO) (Ref. 35 and 36) and La-doped Bi-2201 (Ref. 37). It has also been observed in electron-underdoped $Nd_{2-x}Ce_xCuO_4$ (NCCO) (Ref. 38) and $Pr_{2-x}Ce_xCuO_4$ (PCCO) (Ref. 39). Very recently, this issue has been studied systematically again on a series of high-quality LSCO samples,[40] and the earlier results have been reconfirmed. Quite a few physicists consider this crossover as localization due to inhomogeneities. We disagree with this interpretation. In some of these samples, the estimated $k_F\ell \leq 0.1$, where k_F is the Fermi wave vector and ℓ is the elastic mean free path; i.e., the resistivity is well above the Ioffe-Regel limit. This means localization due to disorder effect is irrelevant here.

More importantly, such a MIC has also been observed in a number of superconducting samples when a strong magnetic

field suppresses the superconductivity. It was first found on LSCO, where a strong pulsed magnetic field up to 60 T could suppress superconductivity in samples up to optimal doping.[41,42] Further, a crossover to insulating behavior was found at low temperatures. A similar crossover was also found in La-doped Bi-2201 (Refs. 43 and 44) and electron-doped $Pr_{2-x}Ce_xCuO_4$ (Ref. 39), as well as in Zn-doped YBCO (Ref. 45). Again, the interpretation in terms of localization due to disorder does not work here, since the estimated $k_F\ell \sim 12$–25 at the MIC point in some of these systems, and the resistivity is well below the Ioffe-Regel limit. Ascribing MIC to proximity to the QCP as caused by charge density wave or d-density-wave instabilities[27,28] is not a good explanation, either. While in LSCO the insulating behavior persists up to optimal doping,[41,42] in La-doped Bi-2201 such a behavior stops at 1/8 doping,[44] well below the optimal doping, and no signatures of any stripe phase showed up. Several authors consider the insulating behavior at low temperatures as due to non-Fermi-liquid properties.[46] However, the MIC itself was not addressed in any theoretical considerations known to us.

In our view the MIC *is the clue to the understanding of the pseudogap phase*. We consider the MIC in underdoped cuprates in the absence of a magnetic field and MIC in superconducting samples when a strong magnetic field suppresses superconductivity, *the same phenomenon with the same origin*: as an outcome of the competition between the short-range antiferromagnetic order and the dissipative motion of the charge carriers. We have applied the SU(2) $\times$U(1) Chern-Simons (the spin-charge) gauge field theory to treat this problem.[47–49] The formalism itself will be outlined briefly in the next section, whereas here we give some intuitive picture of our main results.

We start from the Mott insulating state which shows antiferromagnetic long-range order (AF LRO). Upon doping beyond certain threshold the AF LRO is destroyed, being replaced by AF short-range order (SRO), characterized by an AF correlation length ξ. Since the holes distort the AF background and their average distance $\sim \delta^{-1/2}$, intuitively, $\xi \approx \delta^{-1/2}$, where δ is the doping concentration. This has been confirmed by the neutron scattering experiments.[50] Our theoretical treatment proves $\xi \approx (\delta|\ln \delta|)^{-1/2}$, providing the first length scale. Put another way, the corresponding energy scale is the spin excitation (spinon) gap $m_s = J(\delta|\ln \delta|)^{1/2}$, where J is the AF exchange interaction. A competing factor is the dissipative motion of the charge carriers with characteristic energy $\sim Tm_h$, where T is the temperature, while $m_h \sim \delta/t$ is the effective mass of the charge carrier (holon), t the hopping integral. The corresponding length scale is the thermal de Broglie wavelength $\lambda_T \sim (T\delta/t)^{-1/2}$. We know that in transport and many related phenomena when two scales are competing producing a crossover, only the shortest time (and corresponding length) scale or the largest energy scale matters. Thus, at low temperatures $\xi \lesssim \lambda_T$, the AF SRO dominates, and the charge carriers become localized, showing insulating behavior. We would like to emphasize that this "peculiar localization" is mainly due to interaction rather than disorder. On the other hand, at high temperatures $\xi \gtrsim \lambda_T$, the dissipative motion of charge carriers dominates,

exhibiting metallic conductivity. Therefore the competition, or fighting between the real part of the "self-energy," the mass gap, and the imaginary part, the dissipation gives rise to this spectacular phenomenon: MIC. In this sense, it serves as a clue to the understanding of the pseudogap phase.

A natural question would be, what are the other consequences of the existence of these two factors? It turns out that a number of experimental observations in the pseudogap phase can be explained by it. Roughly speaking, the spin (spinons) and charge (holons) excitations in the pseudogap phase behave like "separate particles" in their scattering against gauge fluctuations, which renormalizes their properties and dominates the in-plane transport phenomena. However, at small energy-momentum scale the gauge field binds spinon and antispinon into magnon "resonance." Similarly spinon and holon are bound into electron "resonance" with non-Fermi-liquid properties. In particular, these "recombined" particles show up in the out-of-plane transport.

D. Outline of the rest of the paper

The formulation of the spin-charge gauge field theory was presented earlier.[47] The calculation of the in-plane resistivity and MIC in underdoped cuprates in the absence of magnetic field was briefly reported in Ref. 48, whereas the MIC in superconducting samples when a strong magnetic field suppresses superconductivity was considered in Ref. 49. Due to space limitations, the presentation in these two publications was inevitably too concise. The main purpose of this paper is twofold: to present the computations in more detail to outline the essential steps and to compare the results of our calculation with experiments in the pseudogap phase in a more systematic way. Most results have not been published before.

The spin-charge gauge formalism is outlined in Sec. II, whereas the calculation of the in-plane and out-of-plane resistivity is described in Sec. III. The computation of the "spinon" current-current correlation function which is the key ingredient in studying many physical quantities is presented in Sec. IV. The calculation of the Green's function for the physical electron needed to compare with the ARPES data and FS, as well as the c-axis resistivity calculation, is described in Sec. V. In our approach the spin and charge are not fully separated, as in one-dimensional interacting systems. They are not confined, either. Instead, they form a bound state due to the transverse gauge field. A new energy scale—the inverse recombination time for the physical electron—appears in the binding process which shows up in the out-of-plane resistivity. Section VI is devoted to comparison of theory with experiment. We first start with the in-plane resistivity (A), whose normalized value shows universal behavior (B), then continue with out-of-plane resistivity (C). Finally, we consider other observables, including the magnetoresistance (D) and the spin-lattice relaxation rate (E). The paper ends with several concluding remarks (Sec. VII).

II. SPIN-CHARGE GAUGE FORMALISM

In this section we review the formalism involved in the derivation of the low-energy effective action for the t-J

model in a range of parameters which should provide an adequate theoretical description of the "pseudogap phase" of high-T_c cuprates. This effective action will be the starting point for the computation of physical observables to be compared with the experimental data. For further details on the derivation, see Ref. 47.

A. Chern-Simons representation of the *t-J* model

Our theoretical treatment of the *t-J* model is based on the following theorem.[47,51]

If we couple the fermions of the *t-J* model to a U(1) gauge field B_μ, gauging the global charge symmetry, and to an SU(2) gauge field V_μ, gauging the global spin symmetry of the model, and we assume that the dynamics of the gauge fields is described by the Chern-Simons actions:

$$S_{c.s.}(B) = -\frac{1}{2\pi} \int d^3x \, \epsilon^{\mu\nu\rho} B_\mu \partial_\nu B_\rho,$$

$$S_{c.s.}(V) = \frac{1}{4\pi} \int d^3x \, \text{Tr} \, \epsilon^{\mu\nu\rho} \left[V_\mu \partial_\nu V_\rho + \frac{2}{3} V_\mu V_\nu V_\rho \right], \quad (1)$$

where $\epsilon^{\mu\nu\rho}$ is the fully antisymmetric tensor; then the spin-charge [or SU(2)×U(1)] gauged model so obtained is exactly equivalent to the original *t-J* model.

Let us give some ideas of the proof of the above theorem for the partition function. We expand the partition function of the gauged model in the first-quantized formalism in terms of the world lines of fermions. After integrating out the gauge fields, the effect of the coupling to $B_\mu(V_\mu)$ is only to give a factor $e^{-i\pi/2}(e^{i\pi/2})$ for any single exchange of the fermion world lines, so the two effects cancel each other exactly.

To the fermion field of the gauged model, denoted by χ_α (α spin index), we apply a formal spin-charge decomposition: $\chi_\alpha \sim H z_\alpha$, where H denotes a spinless fermion (holon) field and z_α a spin-$\frac{1}{2}$ hard-core boson (spinon) field satisfying the constraint $z_\alpha^* z_\alpha = 1$. This constraint eliminates double occupation, as required in the *t-J* model.

The above spin-charge decomposition introduces a further U(1) gauge symmetry which will be called h/s (from holon/spinon):

$$z_\alpha(x) \rightarrow e^{i\Lambda(x)} z_\alpha(x), \quad H(x) \rightarrow H(x) e^{-i\Lambda(x)}, \quad (2)$$

with Λ a real gauge parameter, with which a self-generated gauge field A_μ is associated, analogous to the one appearing in the slave boson and slave fermion approaches.[21,22]

We remark that, in view of this residual h/s gauge interaction, the spin-charge separation performed above is *a priori* purely formal and only the dynamics of the coupled system determines if it has a physical substance. As an example, a confining dynamics would completely destroy the physical spin-charge separation.

In a mean-field approximation[47] (MFA) to the spin-charge gauged *t-J* model, in a region of parameters which should correspond to the "pseudogap phase" of high-T_c cuprates, the role of the three gauge fields is the following.

(i) B_{MFA} carries a flux π per plaquette, converting via the Hofstadter mechanism the spinless holon H into a Dirac fermion, with linear dispersion and a pseudospin structure related to the two Néel sublattices. The fermion system exhibits a "small" FS with $\epsilon_F \sim t\delta$, δ being the doping concentration, centered around the points $(\pm\pi/2, \pm\pi/2)$ in the Brillouin zone.

(ii) V_{MFA} dresses the holons by spin vortices of opposite chirality in the two Néel sublattices. The spinons in the presence of this gas of "slowly moving" dressed holons acquire a mass $m_s \sim \sqrt{\delta|\ln\delta|}$ yielding SRAFO. This is due to a coupling at large scales of the form $(V_{MFA}^2 z_\alpha^* z_\alpha)$. Self-consistency of this treatment relies on the inequality $\epsilon_F \sim t\delta \ll \epsilon_s \sim J\sqrt{\delta|\ln\delta|}$ for small δ. The derived doping dependence of the AF correlation length is consistent with the neutron data.[50]

(iii) The self-generated "photon" field A_μ couples the Fermi liquid of holons to the gapped spinons, described by a massive (CP^1) nonlinear sigma (NLσ) model.

B. Magnons and electrons as "composite" particles

A low-energy effective action for A is obtained by integrating out spinons and holons, in a path-integral formulation. We make the assumption that the scaling limit (large distance, long time) can be taken separately for the two subsystems.[52] Then, using the techniques of Ref. 53, one can prove that in this scaling limit the action is *quadratic* in A. This conclusion follows from a derivative expansion for the spinon action, due to the presence of a mass scale m_s, and from a tomographic decomposition along rays perpendicular to the FS of holons, using the quadratic dependence on A of the scaling action for a single ray (Schwinger action). This means that all results derived from the renormalized *quadratic* action in A are valid beyond the standard perturbative treatment. Thus the skepticism towards the gauge field approach based on the worry that the coupling to the gauge field is strong, while the treatment is perturbative, is not well justified.

The term obtained from spinon integration is a two-dimensional (2D) Maxwell-like action (as in quantum electrodynamics), because the spinons are massive and the spinon action is parity invariant. The transverse component would then generate a logarithmic confining potential between spinons and anti-spinons. The longitudinal part is gapped due to the plasmon effect at finite T. This means that if only spinons were coupled to the gauge field, the renormalized gauge field would have confining dynamics. However, there are also fermions (holons) coupled to the gauge field, as well. The term obtained from holon integration, due to the presence of a finite FS, exhibits a Reizer singularity.[55] More precisely, the transverse component A^T of the gauge field turns out to be, for $\omega, |\vec{q}|, \omega/|\vec{q}| \sim 0$, of the form

$$\langle A^T A^T \rangle(\omega, \vec{q}) \sim \left(-\chi|\vec{q}|^2 + i\kappa \frac{\omega}{|\vec{q}|} \right)^{-1}, \quad (3)$$

where χ is the diamagnetic susceptibility and κ the Landau damping.

This behavior dominates over the Maxwellian term at large scales, destroying confinement. Nevertheless, as we

shall see, the attraction generated by A^T in spinon-antispinon and spinon-holon pairs will be sufficient to produce resonances with the quantum numbers of the magnon and electron, respectively. Therefore a true spin-charge separation is not realized in our approach. An "intermediate" situation in between confinement and full separation—namely, the "*composite*" *nature of magnons and electrons*—is at the root of our interpretation of the anomalous behavior of physical quantities.

A key and novel feature of our approach is the mass of the spinon with a specific doping dependence described above. This feature is not shared by the other SU(2)×U(1) gauge field theory[23] where the gauged SU(2) symmetry is an enlargement of the particle-hole symmetry at half-filling with switched statistics of holon and spinon with respect to ours. The mass of the spinons in our approach and its competition with dissipation of the gauge field due to coupling with holons have far-reaching consequences, and it turns out to be responsible, in our scheme, for phenomena like the MIC, the low-T positive transverse in-plane magnetoresistance, the peak in the dc conductivity, and the Cu spin-lattice relaxation rate, hence for many experimental signatures of the "pseudogap phase."

C. Motivation for the gauging group choice

We end this section with some comments on our choice of the gauging group in the theorem stated at the beginning of this Section. This theorem is a special case of the following more general theorem.

Theorem[56] (Chern-Simons representations of the *t-J* model). Let G be a subgroup of the global symmetry group of the 2D *t-J* model; consider the G-gauged *t-J* model obtained by replacing the fermion field, c, of the *t-J* model in the action, $S_{tJ}(c)$, with a new field χ minimally coupled to a gauge field W, with gauge group G. Denote the action of the G-gauged model by $S_{tJ}(\chi, W)$. Define the Chern-Simons action for W by

$$S_{c.s.}(W) = \frac{1}{4\pi} \int d^3 x \, \mathrm{Tr} \, \epsilon^{\mu\nu\rho} \left[W_\mu \partial_\nu W_\rho + \frac{2}{3} W_\mu W_\nu W_\rho \right].$$

Then, for a suitable choice of a real constant k_G and of the statistics of χ, fermionic or bosonic depending on k_G, the model with action $S_{tJ}(\chi, W) + k_G S_{c.s.}(W)$ is exactly equivalent to the original *t-J* model.

The two basic features of the 2D *t-J* model needed for the proof of the theorem are its dimensionality, necessary to apply the Chern-Simons theory, and the Gutzwiller projection forbidding double occupation, needed to have at most point-like intersection between χ world lines. In fact (see the comment after the theorem in Sec. II A), only with this property can we associate well-defined phase factors to interchange of the world lines.

Each of the Chern-Simons representations allowed by the theorem can be taken as a starting point for a mean-field theory. In particular the slave boson and slave fermion approaches can be derived by choosing $G = $U(1) and $k_{U(1)} = +1$ and -1, respectively.[51] Our choice of the SU(2) ×U(1) spin-charge gauging is motivated by the analysis of the 1D *t-J* model in the limit of small J/t.[57] The model is exactly solvable by Bethe ansatz and conformal field theory techniques, and one knows the critical exponents of its correlation functions. They are basically derived by decomposing the fermion field of the model into spinon and holon. The spin-charge gauging corresponds, using a dimensional reduction from 2D to 1D, to a semionic nature of the two excitations; i.e., an exchange of spinon or holon fields yields phase factors $e^{\pm i\pi/2}$, intermediate between the fermionic $e^{i\pi}$ and the bosonic 1. This is exactly a property needed to reproduce, in a sort of MFA, the known critical exponents. It may be worthwhile to compare the role of the U(1), SU(2), and h/s gauge fields in 1D and 2D. In 1D a gauge field has no transverse (physical) components, while in 2D it does have one. The disappearance of this degree of freedom in 1D with respect to 2D induces the following effects.

(i) $B^T_{MFA} = 0$; hence there is no Hofstadter mechanism and the holon has a quadratic dispersion.

(ii) $V^T_{MFA} = 0$; hence there is no spinon mass generation.

(iii) $A^T_\mu = 0$; hence spinons and holons are decoupled and this yields a true spin-charge separation in 1D.

III. RESISTIVITY AND SPIN-CHARGE DECOMPOSITION

In this section we highlight the distinctive features of the experimental data on in-plane and out-of-plane resistivity in underdoped cuprates, sketch the theoretical scheme for computations, and outline the qualitative understanding of the resistivity behavior in our gauge field approach.

A. In-plane resistivity

One of the first striking experimental findings on high-T_c cuprates was the anomalous behavior of in-plane resistivity, which in optimally doped samples appears linear in T. In underdoped samples, it deviates from the linear dependence at low temperatures, but the standard metallic behavior $\sim T^2$ derived from the Fermi liquid theory is not observed. Instead, there are the following two distinctive features.

(a) In many strongly underdoped samples there exists a minimum in the resistivity, around ~ 50–100 K, corresponding to a MIC, as we outlined in Sec. I C. A similar crossover is also observed in superconducting samples if superconductivity is suppressed by applying a strong magnetic field.

(b) Another characteristic feature of in-plane resistivity which appears quite universal in underdoped samples is an inflection point—i.e. a maximum of $d\rho/dT$ at T^* ~ 100–300 K; this maximum disappears for higher dopings. At even higher temperatures the resistivity exhibits a linear in T behavior approached from below. In the literature T^* is also defined by some authors as the temperature where the resistivity deviates from the linear dependence, as we mentioned in Sec. I A. That value is higher than the inflection point.

To calculate the in-plane resistivity we use the Ioffe-Larkin rule,[21] a somewhat counterintuitive but a typical feature of the gauge approach, stating that the physical resistivity ρ is a sum of the resistivity due to spinons, ρ_s, and the resistivity due to holons, ρ_h:

$$\rho = \rho_s + \rho_h . \qquad (4)$$

The derivation of this addition rule is based on the following consideration: If we couple the electron to an external electromagnetic (e.m.) field $A_{e.m}$, it turns out that we can attribute an arbitrary e.m. charge ϵ with $0 \le \epsilon \le 1$ to the spinon and a charge $1 - \epsilon$ to the holon, because in the path integral formalism, ϵ can always be eliminated by the change of variable $A \to A + \epsilon A_{e.m}$. As a consequence, neglecting "photon" drag, the renormalized e.m. current polarization bubble $\Pi_{e.m.}$ obeys the rule

$$(\Pi_{e.m.})^{-1} = (\Pi_s)^{-1} + (\Pi_h)^{-1} . \qquad (5)$$

From Eq. (5) and the Kubo formula, one can derive the Ioffe-Larkin rule, provided both conductivities σ_s and σ_h are non-vanishing. This will be self-consistently verified *a posteriori* except for very low temperatures. A crucial assumption here is the quadratic dependence of the effective action in A, which, as we pointed out in Sec. II A, is valid beyond the standard perturbation expansion in the scaling limit. So does the Ioffe-Larkin formula.

Denoting by j^s the spinon current, the spinon resistivity is calculated from the fully renormalized current polarization bubble

$$\langle j^s(x) j^s(y) \rangle = \Pi_s(x - y) \qquad (6)$$

via the Kubo formula

$$(\rho_s)^{-1} = \sigma_s = -[\omega^{-1} \mathrm{Im}\, \Pi_s^R(\omega, \vec{q} = 0)]|_{\omega \to 0}$$

$$= 2 \int_0^{\infty} dx^0 x^0 \Pi_s(x^0, \vec{q} = 0) . \qquad (7)$$

For holons we have similar equations replacing the index s by h (e.g., j^h denotes the holon current). In Eq. (6) the expectation value is taken by integration over A, the spinon field z_α of the continuum NLσ model, and the Dirac holon field ψ. The last equality in Eq. (7) is obtained via the Lehmann representation and the superscript R denotes the retarded propagator.

As pointed out first by Anderson,[18] the in-plane resistivity should be interpreted in terms of spin-charge separation. In a gauge approach, if the scattering time of spinons or holons by gauge fluctuations is shorter than the lifetime of the electron (as in our case), then this time scale will dominate the in-plane resistivity and it might exhibit a different temperature dependence than the electron lifetime.

It turns out that a peculiar feature like MIC is mainly due to the spinon contribution. As we mentioned in Sec. I C, MIC is caused by competition between the spinon mass term with the gauge field dissipation. The spinon contribution to resistivity, proportional to the spinon scattering rate against the gauge field, turns out to be $\sim T^{-1}$ at low temperatures when the spinon mass effect dominates, while it is $\sim T^{1/4}$ at high temperatures when the gauge field dissipation overwhelms.

In our theoretical framework we identify the inflection point as the signal of a crossover to a different "phase," the so-called strange-metal phase, characterized by T-linear resistivity, which will be addressed in a separate paper.[58] More-over, as will be shown in Sec. VI B, the normalized resistivity is a universal curve if its value at the MIC point T_{MIC} and the inflection point T^* are used as references. At very low temperature many samples exhibit a second inflection point below which the resistivity appears approximately logarithmic in T (Ref. 41); again we interpret this as a crossover to a different "phase."

B. Out-of-plane resistivity

The out-of-plane resistivity exhibits a completely different T dependence. At low temperatures in the "pseudogap phase" ρ_c is insulating, behaving like T^{-1} with a coefficient essentially independent of the material.[18] At higher temperatures ρ_c typically develops a rounded knee.[59,60] As emphasized by Anderson,[18] the coexistence at the same temperature of a metallic in-plane and an insulating out-of-plane resistivity is hard to reconcile within a Fermi liquid theory, whereas it might have a natural explanation in the framework of spin-charge "separation." In such a scheme, in fact, a spinon-holon decomposition of the electron holds only in the CuO_2 layer and spinons and holons should recombine into electrons to hop between layers and contribute to ρ_c. The out-of-plane resistivity is then determined by the time scale of electron recombination. In our approach we have a way to implement this general ideas proposed by Anderson in the "pseudogap phase."

To calculate ρ_c we use the approach proposed by Kumar and Jayannavar[61] (KJ) which is motivated by the experimental observation that the c-axis transport is essentially incoherent; i.e., there is no bandlike motion orthogonal to the CuO_2 planes. One can then consider a system of two layers weakly coupled by an effective tunneling matrix element $-t_c$, taking into account an averaged momentum dependence of the hopping parameter (vanishing for diagonal momenta). One can write the 2D retarded Green function of the electron (holon-spinon) resonance for small ω and momentum $\vec{k}_F$ on the FS as

$$G^R(\omega, \vec{k}_F) \sim \frac{Z}{\omega + i\Gamma} , \qquad (8)$$

where Z is the wave function renormalization and Γ the scattering rate. Taking into account a virtual hopping between two layers induces a shift of the real part of the denominator of Eq. (8) from ω to $\omega \pm Z t_c$. Let us denote by $G_\pm^R$ the corresponding Green's functions. The out-of-plane conductivity in the incoherence regime can be written through the Kubo formula as

$$\sigma_c = -\sum_{\vec{k}} \int \frac{d\omega}{2\pi} 2 t_c^2 e^2 \frac{\partial n}{\partial \omega}(\omega) A_+(\vec{k}, \omega) A_-(\vec{k}, \omega), \quad (9)$$

where $A_\pm = (-1/\pi) \mathrm{Im}\, G_\pm$ are the spectral functions and $n(\omega)$ the Fermi distribution function. Inserting Eq. (8) into Eq. (9) after standard manipulations one obtains

$$\rho_c \sim \frac{1}{\nu} \left(\frac{1}{\Gamma} + \frac{\Gamma}{t_c^2 Z^2} \right), \qquad (10)$$

where ν is the density of states at the FS. One can already anticipate that the first term causes the insulating behavior and, being independent of t_c, it is essentially independent of the material, as experimentally observed. Via Eq. (10) we have related the behavior of ρ_c to the computation of Γ and Z, thus to the low-energy behavior of the electron Green function. This propagator in turn can be expressed at large scales in terms of holon and spinon fields z_α and ψ_σ and be extracted from a linear combination of terms

$$\langle \psi_\sigma(x) z_\alpha^*(x) \bar{\psi}_\sigma(y) z_\alpha(y) \rangle, \tag{11}$$

where σ denotes the pseudospin structure of the Dirac holons, α the component-spin index of the spinons, and the propagator (11) is calculated using the low-energy spinon and holon effective actions.

We shall see that the *derived* lifetime of the electron resonance is $\sim T^{-1}, T^{-1/2}$ at low and high temperatures, respectively, and therefore it cannot explain the temperature behavior of in-plane resistivity, in particular the MIC, but it indeed sets the scale of the out-of-plane resistivity. We shall also see that the theoretical curve indeed has a rounded knee, corresponding to the crossover between the high- and low-temperature regimes, in full consistency with experiment.

The following two sections (IV and V) are more technical. Those who are mainly interested in the qualitative aspect of the gauge field approach can skip them and move directly to Sec. VI.

IV. SPINON CURRENT-CURRENT CORRELATION FUNCTION

In this section we outline the computation of the spinon current polarization bubble—i.e., the current-current correlation function $\Pi_s(\omega, \vec{q})$—at small ω and $\vec{q}$. This computation was briefly sketched in Ref. 48 and it is needed to derive the in-plane resistivity, as explained above. We will provide more technical details here for those who would like to follow the actual calculation.

A. Feynman-Schwinger-Fradkin representation

We start by writing explicitly the spinon NLσ model effective action

$$S = \int d^3x \frac{1}{g} [v_s^{-2} |(\partial_0 - iA_0) z_\alpha|^2 + |(\partial_i - iA_i) z_\alpha|^2 + m_s^2 z_\alpha^* z_\alpha,], \tag{12}$$

where $g \sim J^{-1}$, $v_s \sim Ja$ is the spinon velocity, with a the lattice spacing, and $m_s^{-1} \sim a/(|\delta \ln \delta|)^{1/2}$ the spinon correlation length. After a suitable rescaling of variables, the spinon propagator can be recast in the Schwinger representation

$$G_\alpha(x, y|A) = ig v_s \int_0^\infty ds \, e^{-is(\Delta_A + m_s^2)}(x, y), \tag{13}$$

where $x = (v_s x^0, \vec{x})$, $A = (v_s A_0, \vec{A})$, and Δ_A denotes the 3D covariant Dalambertian (or relativistic Laplacian). The propagator has been considered in the zero-temperature for-

malism, an approximation justified by the mass gap of the spinon. Roughly speaking, it is valid provided $T \ll Jam_s \sim J(|\delta \ln \delta|)^{1/2}$. The kernel appearing in Eq. (13) has the formal structure of an evolution kernel for a 3D Hamiltonian $H = -\Delta_A + m_s^2$ and time parameter s. It can thus be expanded in terms of Feynman paths starting from y at "time" 0 and reaching x at "time" s. It is convenient to parametrize these paths through their three-velocity ϕ^μ, $\mu = 0, 1, 2$, using a Feynman-Schwinger-Fradkin (FSF) representation (see, e.g., Ref. 62)

$$G_\alpha(x, 0|A) = ig v_s \int_0^\infty ds \, e^{-ism_s^2} \int \mathcal{D}\phi \int d^3p$$

$$\times \exp\left[ip\left(\int_0^s \phi(t)dt - x \right) \right]$$

$$\times \exp\left\{ i \int_0^s dt \left[\tfrac{1}{4} \phi^2(t) \right. \right.$$

$$\left. \left. + \phi \cdot A\left(x + \int_0^t \phi(t')dt' \right) \right] \right\}. \tag{14}$$

Here the p integration enforces the constraint on the initial and final points of the paths and we use a shorthand notation for the 3D scalar product: e.g.,

$$p \cdot x = p_\mu x^\mu. \tag{15}$$

For a better understanding of formula (14), notice that formally setting $\phi^\mu(t) = dx^\mu(t)/dt$, the last exponential is i times the Lagrangian of a 3D particle coupled to the e.m. potential A_μ, corresponding to the previous Hamiltonian H, as one expects in a path-integral formulation. Since under a h/s gauge transformation $\Lambda(x)$ the spinon field $z_\alpha(x)$ changes by the phase factor $e^{i\Lambda(x)}$, it follows that

$$G_\alpha(x, 0|A_\mu + \partial_\mu \Lambda) = e^{i[\Lambda(x) - \Lambda(0)]} G_\alpha(x, 0|A_\mu). \tag{16}$$

The gauge dependence of the Green function is already captured by the so-called "Gor'kov approximation"

$$G_\alpha(x, 0|A) = \exp\left(i \int_0^x A_\mu dx^\mu \right) G_\alpha(x, 0), \tag{17}$$

where $\int_0^x$ denotes integration along a straight line from 0 to x and $G_\alpha(x, 0)$ is the free propagator (in the absence of gauge field). Expression (14) is useful to go beyond Gor'kov approximation by means of the identity[62]

$$\int_0^s A_\mu\left(x + \int_0^t \phi(t')dt' \right) \phi^\mu(t)dt$$

$$= \int_0^x A_\mu dx^\mu - \int_0^1 d\lambda \lambda \int_0^s dt \int_0^t dt' \, \phi^\mu(t) \phi^\nu(t')$$

$$\times F_{\mu\nu}\left(x + \lambda \int_0^t \phi(t'')dt'' \right), \tag{18}$$

where $F_{\mu\nu} = \partial_\mu A_\nu - \partial_\nu A_\mu$ is the gauge field strength. Pictorially, this representation is illustrated in Fig. 1. The second

FIG. 1. Feynman-Schwinger-Fradkin representation.

term in Eq. (18), denoted by $\Sigma(P)$, gives the correction to the Gor'kov approximation and it is gauge invariant, as it depends only on $F_{\mu\nu}$. Shifting $\phi^\mu(t)$ by $2p^\mu$ one can rewrite

$$G_\alpha(x,0|A) = \exp\left(i \int_0^x A_\mu dx^\mu \right) G_\alpha(x,0|F), \qquad (19)$$

$$G_\alpha(x,0|F) = igv_s \exp\left(i \int_0^x A(\xi)d\xi \right) \int_0^\infty ds \int \frac{d^3p}{(2\pi)^3}$$

$$\times \exp[-ipx - i(p^2 + m_s^2]$$

$$\times \int \mathcal{D}\phi \exp\left(i\frac{1}{4} \int_0^s dt\, \phi^2(t) \right)$$

$$\times \exp\left[-i \int_0^1 d\lambda\, \lambda \int_0^s ds' \int_0^{s'} ds''[\phi^\mu(s') \right.$$

$$- 2p^\mu][\phi^\nu(s'') - 2p^\nu]$$

$$\times F_{\mu\nu}\left(\lambda \int_0^{s'} [\phi(s''') - 2p]ds''' \right) \Big]. \qquad (20)$$

B. Gauge field strength F correlation function

Now we turn to the polarization operator Π_s. Expressing it in terms of spinon propagators we find

$$\Pi_s(x,y) = \langle D_{A(x)} G(x,y|A) D^\dagger_{A(y)} G(y,x|A) \rangle_A$$

$$= \left\langle \left(\partial_\mu - \frac{i}{2} \int_y^x F_{\mu\nu} dx^\nu \right) G(x,y|F) \right.$$

$$\times \left(\partial^\mu - \frac{i}{2} \int_y^x F^{\mu\rho} dx_\rho \right) G(x,y|-F) \right\rangle_A, \qquad (21)$$

where $\langle \cdot \rangle_A$ denotes integration over A with the effective action in the scaling limit and D_A the covariant derivative. Notice that the two non-gauge-invariant Gor'kov terms of the two spinon propagators cancel each other so that the result is explicitly gauge invariant and it depends only on F. We use now the quadratic structure of the scaling action $S(A)$ (see Sec. II B) to integrate out the gauge field. The explicit expression for $S(A)$ in the Coulomb gauge is

$$S(A) = \frac{1}{2} \int dx^0 d^2x\, A_\mu \tilde{\Pi}^{\mu\nu} A_\nu,$$

with nonvanishing polarization components in the limit of small ω, $\vec{q}$, and $\omega/|\vec{q}|$, where one finds the leading, Reizer singularity, given by[55]

$$\tilde{\Pi}^\perp_{ij}(\vec{q},\omega) = \left(\delta_{ij} - \frac{q_i q_j}{q^2} \right)\left[-i\kappa \frac{\omega}{|\vec{q}|} + \chi |\vec{q}|^2 \right], \quad i,j = 1,2,$$
$$\qquad (22)$$

$$\Pi_{00}(\vec{q},\omega) = \nu + \omega_p. \qquad (23)$$

In Eqs. (22) and (23), $\chi = \chi_s + \chi_h$, where $\chi_{s(h)}$ is the spinon (holon) diamagnetic susceptibility, κ the Landau damping, ν the density of states at the FS of holons, and ω_p the plasmon gap. For free holons,

$$\chi_h = \frac{1}{12\pi m_h} \sim \frac{t}{6\pi\delta}, \qquad (24)$$

and for free spinons,

$$\chi_s \sim m_s^{-1}. \qquad (25)$$

Hence, in this presumably reasonable approximation, for low doping $\chi_h \gg \chi_s$. Due to the dependence on the field strength F in Eq. (21), only the correlator of the electric (F_{0i}) and magnetic (F_{ij}) fields can appear in the computation. Since the A_0 propagator is short ranged whereas the A^T propagator is long ranged, the "electric" field contribution at large scales is negligible with respect to the "magnetic," and in first approximation we neglect it. However, it might be useful to keep in mind that doing this we neglect a short-range attraction between spinon and antispinon (or holon). Due to the gapless nature of A^T, we consider the effect of finite temperature using the thermal propagator

$$\langle F_{ij}(x) F_{rs}(0) \rangle$$

$$= (\delta_{ir}\delta_{js} - \delta_{is}\delta_{jr}) \int \frac{d\omega}{2\pi} \int \frac{d\vec{k}}{(2\pi)^2} \frac{|\vec{k}|^2 e^{-i\omega\xi^0 + i\vec{k}\cdot\vec{\xi}}}{i\frac{\omega}{|\vec{k}|}\kappa - \chi|\vec{k}|^2}$$

$$\times \coth\left(\frac{\omega}{2T} \right). \qquad (26)$$

This does not contradict our earlier approximation in considering the zero-temperature spinon propagator in view of the finite spinon mass gap. The leading order in T correction enters via the thermal gauge field propagator in our scheme. Since the energy scale for field fluctuations is set by T, in Eq. (26) the integration over frequency is cut off at $\omega \lesssim T$ which in turn implies $|\vec{k}| \lesssim (T\kappa/\chi)^{1/3}$.

In the limit $T\xi^0 \ll 1$ an approximate evaluation of the above integral gives

$$-i\frac{T}{4\pi\chi} Q_0^2 e^{-Q_0^2|\vec{\xi}|^2/4}, \qquad (27)$$

where $Q_0 = (\kappa T/\chi)^{1/3}$ is a momentum cutoff and Q_0^{-1} can be identified as the length scale of gauge fluctuations, analogous

to the anomalous skin depth. (*A posteriori* the upper limit for T in the inequality above turns out to be reasonable because the typical time scale is $\sim Q_0^{-1} \sim T^{-1/3} < T^{-1}$ at low T.) It turns out that this scale is triggering also the size of the spinon-antispinon magnon resonance. It also follows that for $m_s \gg Q_0$ in the expectation value (21) the derivative term dominates over the F terms at large scales, so that to evaluate Π_s the leading term is obtained by computing

$$\langle G(x,0|F) G(x,0|-F) \rangle_A \tag{28}$$

and then taking the spatial derivatives. Notice that Eq. (28) coincides with the propagator $\langle \vec{\Omega}(x) \cdot \vec{\Omega}(0) \rangle$, where $\vec{\Omega} = z^* \vec{\sigma} z$ is a "magnon" field. We denote by ϕ_1^μ and ϕ_2^μ the velocity fields relative to the FSF representation of the two Green functions in Eq. (28). Integrating over A the product of the two FSF expansions one obtains an effective action $I(\phi_1, \phi_2)$ in the velocity fields, which is quartic neglecting the ϕ dependence in F. This approximation can be self-consistently justified *a posteriori*, because [see Eq. (33)]

$$p \sim m_s \gg \frac{1}{s} \int_0^s ds' \, \phi(s') \sim s^{-1/2} \sim (x^0/m_s)^{-1/2}. \tag{29}$$

C. Eikonal and saddle point approximation

The ϕ integration is then performed using the eikonal approximation

$$\int [\mathcal{D}\phi_1][\mathcal{D}\phi_2] \exp\left\{ \frac{i}{4} \int \phi_1^2 + \frac{i}{4} \int \phi_2^2 \right\} e^{I(\phi_1, \phi_2)}$$

$$\simeq e^{i \langle I(\phi_1, \phi_2) \rangle_{\phi_1, \phi_2}}, \tag{30}$$

where $\langle \cdot \rangle_{\phi_1, \phi_2}$ denotes the average with respect to the Gaussian measure appearing in the left-hand side (LHS) of Eq. (30). This can be justified if I is small, since $I \sim T$ for T small. Within this approximation the contribution of the two Green functions factorizes. This factorization in diagrammatic language means that after the cancellation of the self-energy and vertex renormalization implicitly involved in the cancellation among Gor'kov terms, the remaining leading effect of A fluctuations is a self-energy renormalization of the gauge-invariant spinon propagator. At this stage the correlator $\langle \vec{\Omega}(x) \cdot \vec{\Omega}(0) \rangle$ can be written as

$$\left[\int d^3p \int_0^\infty ds \, \exp\left\{ -i\left(p^2 + m_s^2 - \frac{T}{\chi} f(\alpha) \right) s + ipx \right. \right.$$

$$\left. \left. - \frac{T}{\chi} Q_0^2 s^2 g(\alpha) \right\} \right]^2, \tag{31}$$

where $\alpha = |\vec{p}| s Q_0$, f and g are functions which summarize the effect of gauge fluctuations, and their length scale variation is in fact $\sim Q_0^{-1}$. Explicit integral representations of f and g are

$$f(\alpha) = \alpha^2 \int_0^1 d\lambda \lambda \int_0^1 d\tilde{\lambda} \tilde{\lambda} \int_0^1 dv \, v^2 e^{-\alpha^2 v^2 (\tilde{\lambda} - \lambda)^2},$$

$$g(\alpha) = \int_0^1 d\lambda \lambda \int_0^1 d\tilde{\lambda} \tilde{\lambda} \int_0^1 dv \, v e^{-\alpha^2 v^2 (\tilde{\lambda} - \lambda)^2}. \tag{32}$$

Finally we evaluate the p and s integrals by a saddle point approximation, obtaining, for $m_s^2 \gtrsim T/\chi$,

$$p \sim x/2s \quad s \sim \frac{1}{2} \sqrt{ \frac{(x^0)^2 - \vec{x}^2}{m_s^2 - \dfrac{T}{\chi} f(\alpha)} }, \tag{33}$$

and the magnon $\vec{\Omega}$ propagator in x space becomes

$$\langle \vec{\Omega}(x) \cdot \vec{\Omega}(0) \rangle$$

$$\sim \frac{1}{(x^0)^2 - |\vec{x}|^2} \exp\left\{ -2i \sqrt{ m_s^2 - \frac{T}{\chi} f\left(\frac{|\vec{x}| Q_0}{2} \right) } \right.$$

$$\times \sqrt{(x^0)^2 - \vec{x}^2} - \frac{T}{2\chi} Q_0^2 g\left(\frac{|\vec{x}| Q_0}{2} \right)$$

$$\left. \times \frac{(x^0)^2 - |\vec{x}|^2}{m_s^2 - \dfrac{T}{\chi} f\left(\dfrac{|\vec{x}| Q_0}{2} \right)} \right\}. \tag{34}$$

To apply the Kubo formula one needs to perform the Fourier transform at $\vec{q} = 0$ of $\langle \vec{j}^s(x) \cdot \vec{j}^s(0) \rangle \sim \langle \partial_\mu \vec{\Omega}(x) \cdot \partial^\mu \vec{\Omega}(0) \rangle$. We consider the region $x^0 \gg |\vec{x}|$ and evaluate the $|\vec{x}|$ integration via a saddle point. Using the form of f and g one finds that the exponent Eq. (34) at large x^0 exhibits a complex saddle point at a scale $|\vec{x}|(x^0) \sim (x^0)^{1/2}$, thus verifying the above assumed inequality with a behavior of a standard diffusion and with argument $\pi/4$. (In the more precise numerical evaluation we neglect small-scale fluctuations, splitting the above saddle point into a set of isolated saddle points.) A numerical extrapolation in the region of small x^0 yields an approximate x^0 dependence of the form

$$|\vec{x}|(x^0) \sim e^{i\pi/4} x_c(x^0), \quad x_c(x^0) = (C^2 Q_0^{-2} + C' |x^0|/m_s)^{1/2}, \tag{35}$$

with C, C' finite positive constant ($C \sim 0.5$), thus approaching a finite value as $x^0 \to 0$. Setting $\alpha(x^0) = Q_0 |\vec{x}|(x^0)$ and

$$I(x^0) = -i \sqrt{ m_s^2 - \frac{T}{\chi} f(\alpha(x^0)) } x^0$$

$$- \frac{T}{4\chi} Q_0^2 g(\alpha(x^0)) \frac{(x^0)^2}{m_s^2 - \dfrac{T}{\chi} f(\alpha(x^0))}, \tag{36}$$

we have

$$\langle j_\mu j^\mu \rangle (\vec{q} = 0, x^0)$$

$$= \int d^2\vec{x} \langle j_\mu(x^0, \vec{x}) j^\mu(0, \vec{0}) \rangle$$

$$\sim \frac{x_c^3}{[(x^0)^2 - x_c^2]^3} \left(\frac{\partial^2 I(x^0)}{\partial x_c(x^0)^2} \right)^{-1/2} e^{2I(x^0)}. \quad (37)$$

Since f is smooth on the scale $|\vec{x}| \sim Q_0^{-1}$, assuming for x^0 the same scale the dominance of the saddle point requires a lower bound for the temperature, which combined with previous upper bound yields a range of validity given by

$$m_s^2 \gtrsim \frac{T}{\chi} \gtrsim m_s Q_0. \quad (38)$$

In physical units, this gives a range of temperatures between a few tens and a few hundreds of kelvin. The real part of the exponential in Eq. (37) is monotonically decreasing in x^0; therefore we evaluate the x^0 integral appearing in Kubo formula (7) by principal part evaluation. Since our approach is valid only at large scales, we introduce an UV cutoff in the integral at λQ_0^{-1} and evaluate the integration assuming λ large. Then we make the conjecture that for small ω the physics is dominated by large scales and the small-scale contribution can be taken into account by removing the UV cutoff after a multiplicative scale renormalization. The result of this approximation is

$$\sigma_s = 2 \operatorname{Im} \int_0^\infty dx^0 x^0 \Pi(x^0, \vec{q} = 0)$$

$$\sim \operatorname{Im} \left(\frac{Z_j}{\sqrt{m_s^2 - \dfrac{T}{\chi} f(Ce^{i\pi/4})}} \right), \quad (39)$$

where

$$Z_j = Q_0 Z_\Omega, Z_\Omega = (m_s^2 - icT/\chi)^{1/4} [\chi/Tf''(Ce^{i\pi/4})]^{1/2} Q_0^{1/2},$$

and numerically one finds $f(Ce^{i\pi/4}) \sim 0.2 + i3.3$ and $f''(Ce^{i\pi/4})$ real. For simplicity we set $\operatorname{Im} f(Ce^{i\pi/4}) = c$ and we still denote by m_s^2 the quantity $m_s^2 - \operatorname{Re} f(Ce^{i\pi/4}) T/\chi$ which in the range of temperature we are interested is in fact almost equal to m_s^2.

D. Spinon-antispinon "resonance" (magnon) propagator

For a better understanding of the above equation, we notice that the retarded magnon correlator at positive ω is given in the same approximations by

$$\langle \vec{\Omega} \cdot \vec{\Omega} \rangle (\omega, \vec{q}) \sim \frac{Z_\Omega}{\omega - 2\sqrt{m_s^2 - ic\dfrac{T}{\chi}}} J_0(|\vec{q}| C Q_0^{-1} e^{i\pi/4}), \quad (40)$$

where J_0 is the Bessel function.

The above formula explains the physics underlying Eq. (39): the gauge fluctuations couple the spinon-antispinon pair into a resonance with mass gap

$$m_\Omega = 2 \operatorname{Re} \sqrt{m_s^2 - ic\frac{T}{\chi}} \quad (41)$$

and inverse lifetime

$$\tau_\Omega^{-1} = 2 \operatorname{Im} \sqrt{m_s^2 - ic\frac{T}{\chi}}. \quad (42)$$

Z_j and Z_Ω can be interpreted as T-dependent wave-function renormalization factors which modify the temperature dependence of the (physical) correlation functions. Finally, we expect that the plausible effect of the neglected residual short-range attraction is a further renormalization of the mass gap, but we believe that this does not introduce significant changes.

V. ELECTRON GREEN'S FUNCTION

In this section we evaluate the continuum limit of the electron Green's function within our approach, extracting, in particular, the wave-function renormalization constant Z and the inverse lifetime Γ needed to compute ρ_c in KJ's approach.

A. Holon effective action

In order to have a more systematic derivation, it is worthwhile to start by writing the hopping Hamiltonian for holons, H_{hopp}, neglecting at first the coupling to the h/s gauge field.

Restricting the holon field H to the two Néel sublattices, labeled by A, to which the origin belongs, and B, we have in momentum space

$$H_{hopp} = \sum_{\vec{k}} (H_A^*(\vec{k}) \ H_B^*(\vec{k}))$$

$$\times \begin{pmatrix} 0 & -2t\frac{1}{\sqrt{2}}(\gamma_+ + i\gamma_-) \\ -2t\frac{1}{\sqrt{2}}(\gamma_+ - i\gamma_-) & 0 \end{pmatrix}$$

$$\times \begin{pmatrix} H_A(\vec{k}) \\ H_B(\vec{k}) \end{pmatrix}, \quad (43)$$

where

$$\gamma_\pm = \cos(k_x a) \pm \cos(k_y a), \quad (44)$$

a being the lattice spacing and the sum over $\vec{k}$ running in the reduced Brillouin zone. The eigenvalues of H_{hopp} are given by

$$\epsilon_\pm(\vec{k}) = \pm 2t\sqrt{\cos(k_x a)^2 + \cos(k_y a)^2}; \quad (45)$$

hence they describe double cones with vertices at $(\pm\pi/2, \pm\pi/2)$ in the Brillouin zone.

Since the chemical potential for the holon system is positive, $\mu \sim 2t\delta$, only the ϵ_+ band of the double cones exhibits a FS. For each of these double cones one can identify a

two-component, continuum, Dirac field ψ_α, $\alpha = \uparrow, \downarrow$ describing the low-energy physics of the system. The continuum effective action for holons ψ_α coupled to the h/s field A_μ can be cast in the form

$$S_h(\psi, A) = \int d^3x \, \bar{\psi} [\, \gamma_0(\partial_0 - \mu - iA_0) + v_F \gamma_i(\partial_i - iA_i)\,] \psi,$$
(46)

where $\bar{\psi} = \psi^\dagger \gamma_0$, $\gamma_0 = \sigma_z$, $\gamma_i = (\sigma_y, \sigma_x)$, and $v_F = 2ta$ being the Fermi velocity. The relation between ψ, z and the original electron field c_α in the two sublattices is found to be given—e.g., near the $(\pi/2, \pi/2)$ double cone—by

$$\langle c_\alpha^A(x) c_\alpha^{\dagger A}(0) \rangle \sim e^{i(\pi/2,\pi/2) \cdot \vec{x}} \langle [\bar{\psi}_\downarrow(x) \psi_\downarrow(0)$$
$$- \bar{\psi}_\uparrow(x) \psi_\uparrow(0)] z_\alpha(x) z_\alpha^*(0) \rangle,$$

$$\langle c_\alpha^B(x) c_\alpha^{\dagger A}(0) \rangle \sim e^{i(\pi/2,\pi/2) \cdot \vec{x}} \langle [e^{i\pi/4} \bar{\psi}_\uparrow(x) \psi_\downarrow(0)$$
$$+ e^{-i\pi/4} \bar{\psi}_\downarrow(x) \psi_\uparrow(0)] z_\alpha(x) z_\alpha^*(0) \rangle.$$
(47)

Analogous relations hold near the other three double cones. Note that in the z correlator, the contribution of the spin flips of the "optimal spinon configuration" of Ref. 47 must be taken into account.

B. Tomographic decomposition

In the previous section we evaluated the effect of gauge fluctuations on the z correlator at large scales, using the FSF path-integral representation. An analogous representation is hard to use for the ψ_α correlator because of the finite density of holons. This representation would in fact contain a series of alternating sign contributions, corresponding to an arbitrary number of closed fermion word lines, describing the contributions of the particles in the finite-density ground state, besides the path from 0 to x (see, e.g., Ref. 51). To overcome this difficulty, we apply a dimensional reduction by means of the tomographic decomposition introduced by Luther and Haldane.[63] To treat the low-energy degrees of freedom we choose a slice of thickness $\Lambda = k_F/\lambda$, with $\lambda \gg 1$, in momentum space around the FS of ψ, as shown in Fig. 2.

To simplify the description, we assume a circular FS, an approximation reasonable for low δ (the method applies nevertheless to the general case by considering a Fermi momentum varying along the FS). We decompose the slice in approximately square sectors; each sector corresponds to a quasiparticle field in the sense of Gallavotti-Shankar renormalization[64] (see also Ref. 65). Each sector is characterized by a unit vector $\vec{n}(\theta)$, pointing from the center of the FS to the center of the box, labeled by the angle θ between this direction and the k_x axis. The original momentum $\vec{k}$ inside a given sector is written as
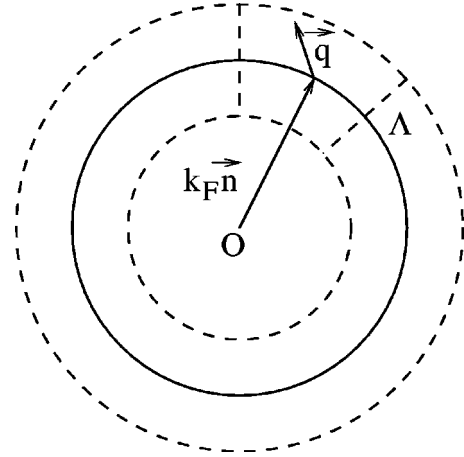
$$\vec{k} = k_F \vec{n}(\theta) + \vec{q},$$
(48)

FIG. 2. Tomographic decomposition of the Fermi surface patch with square boxes of size Λ.

where $\vec{q}$ spans the box; therefore $|\vec{q} \cdot \vec{n}(\theta)|$, $|\vec{q} \wedge \vec{n}(\theta)| \lesssim \Lambda$. Due to the Dirac structure of ψ, to apply the tomographic decomposition to the holon propagator, we first decompose the free ψ correlator as

$$\langle \bar{\psi}_\alpha(x) \psi_\beta(0) \rangle$$

$$= \int \frac{d^3k}{(2\pi)^3} \left[\frac{e^{-ikx}}{-\gamma_0(k_0 + k_F) + \gamma_\mu k_\mu - i\varepsilon \, \mathrm{sgn}(|\vec{k}| - k_F)} \right]_{\alpha\beta}$$

$$= \int \frac{d^3k}{(2\pi)^3} e^{-ikx} \frac{1}{k_0 + k_F - |\vec{k}| + i\varepsilon \, \mathrm{sgn}(|\vec{k}| - k_F)}$$

$$\times \left[\frac{\gamma_0(k_0 + k_F) - \gamma_\mu k_\mu}{k_0 + k_F + |\vec{k}| - i\varepsilon \, \mathrm{sgn}(|\vec{k}| - k_F)} \right]_{\alpha\beta}.$$
(49)

In the scaling limit the matrix in square brackets does not have a pole and, for momenta in a box labeled by $\vec{n}(\theta)$, it approaches

$$A(\theta) = \frac{\gamma_0 - \vec{\gamma} \cdot \vec{n}(\theta)}{2}.$$
(50)

In Ref. 54 it has been shown that the tomographic decomposition is valid at large distances even in the presence of a minimal coupling to a "photon" field. Applying the tomographic decomposition to the holon propagator in the presence of an external h/s gauge field A, in the scaling limit, using Eqs. (49) and (50), we derive

$$\langle \bar{\psi}_\alpha(x) \psi_\beta(0) \rangle$$

$$\sim \sum_i A_{\alpha\beta}(\theta_i) \int \frac{dq_0}{2\pi} \int_\Lambda \frac{d^2q}{(2\pi)^2} e^{-ik_F \vec{n}(\theta_i) \cdot \vec{x}} e^{iq_0 x_0 - i\vec{q} \cdot \vec{x}}$$

$$\times \left[\frac{1}{q_0 - H_{\theta_i} + i\varepsilon \, \mathrm{sgn}[\vec{q} \cdot \vec{n}(\theta)]} \right],$$
(51)

where

$$H_\theta = A_0 + \vec{n}(\theta) \cdot (\vec{q} - \vec{A}) + \frac{1}{2k_F}[(\vec{q} - \vec{A}) \wedge \vec{n}(\theta)]^2, \tag{52}$$

and $\int_\Lambda$ denotes integration over a square box of size Λ. To the Fourier transform of the term in square bracket of Eq. (51) one can apply the FSF path representation (see also Ref. 66 for a treatment of linear dispersion). Using manipulations analogous to those performed in the previous section, one can rewrite Eq. (51) as

$$\frac{k_F}{\Lambda} \int d\theta A(\theta) \exp[-ik_F \vec{n}(\theta)\vec{x}] \exp\left(i \int_0^x A_\mu dx^\mu \right) \int \frac{dq_0}{2\pi} \left[\int_0^\infty du \int_\Lambda \frac{d^2q}{(2\pi)^2} \Theta(q_\parallel) + \int_{-\infty}^0 du \int_\Lambda \frac{d^2q}{(2\pi)^2} \Theta(-q_\parallel) \right]$$

$$\times \exp\{iq^0(x^0-u) - i\vec{q}[\vec{x}+\vec{n}(\theta)u]\} \exp\left(\frac{iq_\perp^2}{2k_F} \right)$$

$$\times \left\{ \int \mathcal{D}\varphi_\perp \exp\left(i \int_0^u \frac{k_F}{2} \varphi_\perp^2(u') du' \right) \exp\left[-i \int_0^1 d\tau \tau \int_0^u du' \int_0^{u'} du'' \varphi^\mu(u') \varphi^\nu(u'') F_{\mu\nu}\left(\tau \int_0^{u'} \varphi(u''') du''' \right) \right] \right\}, \tag{53}$$

where we use the short notation $q_\parallel = \vec{q} \cdot \vec{n}(\theta)$, $q_\perp = \vec{q} \wedge \vec{n}(\theta)$, and φ is the velocity field of components $\varphi^\mu(t) = (1,1,\varphi_\perp(t))$. Note that in Eq. (53) we have replaced the original discrete summation Σ_i with the continuum limit $(k_F/\Lambda)\int d\theta$. We have checked by explicit computation[67] that the term in curly brackets describing the correction to Gor'kov approximation is irrelevant within the approximation scheme adopted in previous section and below, so we shall drop it from now on. (This agrees with the fact that the holon scattering time behaves like $\sim T^{-4/3}$, *a posteriori* a much longer time with respect to the electron scattering time, triggered by gauge fluctuations on spinons.) Then, the u integration can be performed exactly, after the trivial q_0 integration. The $q_\parallel$ integration gives

$$\int_{-\Lambda}^\Lambda dq_\parallel e^{iq_\parallel(x_\parallel - x^0 v_F)} \Theta(q_\parallel)$$

$$= \frac{1}{i} \frac{e^{i\Lambda(x_\parallel - x^0 v_F)} - 1}{(x_\parallel - x^0 v_F)} \sim i \frac{1}{x_\parallel - x^0 v_F}, \tag{54}$$

where the last approximation is valid (in the weak sense) in the limit $\Lambda v_F x^0 \gg 1$. Setting $\Lambda(x_0) = (k_F/v_F x^0)^{1/2}$, the $q_\perp$ integration gives

$$\int_{-\Lambda}^\Lambda dq_\perp e^{i[q_\perp x_\perp - (v_F/k_F)q_\perp^2 x^0]}$$

$$= \Lambda(x_0) \int_{-\Lambda/\Lambda(x_0)}^{\Lambda/\Lambda(x_0)} dy e^{i\Lambda(x_0)x_\perp y} e^{-iy^2/2}$$

$$\sim \Lambda(x_0) \frac{e^{ix_\perp^2 \Lambda(x_0)/2}}{\sqrt{i}}. \tag{55}$$

Collecting all pieces, the holon Green's function in the scaling limit and for $\Lambda x_0 \gg 1$ can be written as

$$\langle \bar{\psi}_\alpha(x) \psi_\beta(0) \rangle$$

$$\sim \frac{\Lambda(x_0)k_F}{\Lambda} \int d\theta \frac{e^{ix_\perp(\theta)^2 \Lambda(x_0)/2}}{\sqrt{i}} A(\theta)_{\alpha\beta} e^{ik_F x \parallel(\theta)}$$

$$\times \left[\frac{1}{x_\parallel(\theta) - x^0 v_F} \Theta(x_0) + \frac{1}{x_\parallel(\theta) + x^0 v_F} \Theta(-x_0) \right]$$

$$\times \exp\left(i \int_0^x A_\mu dx^\mu \right). \tag{56}$$

C. Electron propagator

Next, we compute the electron Green's function using Eq. (47). The Gor'kov terms in the ψ and z correlators cancel against each other and the gauge field fluctuations act only on the gauge-invariant spinon correlator. Within the approximations used in previous section, one can easily verify that this correlator in the scaling limit in x space behaves as square root of the Ω propagator (40). We perform now the Fourier transform of the electron propagator for momenta close to the Fermi surface, in a sector labeled by the angle η, $G_\alpha(\omega,(\pi/2,\pi/2)+\vec{n}(\eta)k_F+\vec{q})$, for small ω and $\vec{q}$. We integrate over θ using the following.

Lemma.[54] Let $f(\theta,\vec{x})$ be a smooth function; then in the large distance limit $|\vec{x}| \gg \Lambda^{-1}$ we have

$$\int d\theta e^{ik_F[\vec{n}(\eta) - \vec{n}(\theta)] \cdot \vec{x}} f(\theta,\vec{x}) \sim \frac{2\pi}{k_F} f(\eta,\vec{x}) \delta_{\Lambda^{-1}}(\vec{x} \wedge \vec{n}(\eta)), \tag{57}$$

where $\delta_{\Lambda^{-1}}$ denotes an approximate δ function of width Λ^{-1}.

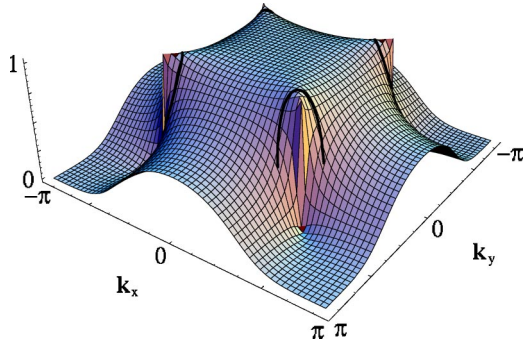Setting $\vec{x} = |\vec{x}|\vec{n}(\phi)$ we approximate

FIG. 3. Angle-dependent spectral weight of the electron propagator. The thick lines close to $(\pm \pi/2, \pm \pi/2)$ represent the region of FS with spectral weight larger than $1/2$ for $\delta \sim 0.05$.

$$\delta_{\Lambda^{-1}}(\vec{x} \wedge \vec{n}(\eta)) \sim \frac{1}{|\vec{x}|} [\delta(\phi - \eta) + \delta(\phi - \eta + \pi)]. \quad (58)$$

One can easily perform the ϕ integration; the remaining integration over space-time variables is done as in the previous section: namely, by saddle point approximation for $|\vec{x}|$ in the limit $x^0 \gg |\vec{x}|$ and by principal part evaluation and scale renormalization for x^0. The final result is

$$G_\alpha \left(\omega, \left(\frac{\pi}{2}, \frac{\pi}{2} \right) + \vec{n}(\eta) k_F + \vec{q} \right)$$

$$\sim S(\eta) Z \left[e^{i\vec{q} \cdot \vec{n}(\eta)|x_c(0)|} \frac{1}{\omega + \Sigma - v_F \frac{d|x_c|}{d|x_0|}(0) q_\parallel} \right.$$

$$\left. + e^{-i\vec{q} \cdot \vec{n}(\eta)|x_c(0)|} \frac{1}{\omega - \Sigma - v_F \frac{d|x_c|}{d|x_0|}(0) q_\parallel} \right],$$

$$(59)$$

where $S(\eta)$ is the angle-dependent part of the wave function renormalization constant:

$$S(\eta) = \frac{1}{2} \left[1 - \frac{1}{\sqrt{2}} [\cos(\eta) + \sin(\eta)] \right]. \quad (60)$$

This angle-dependent spectral weight is demonstrated in Fig. 3. In Eq. (59), Z is the wave function renormalization constant averaged over the FS; writing the tomographic momentum cutoff as $\Lambda = k_F / \lambda$, with $\lambda \gg 1$, and taking into account the definition of Q_0 we obtain

$$Z \approx \lambda \left(\frac{Q_0}{k_F} \right)^{1/2} \left(\frac{m_s \kappa}{J^2} \right)^{1/2}. \quad (61)$$

The renormalized electron self-energy Σ is given by

$$\Sigma = v_s \sqrt{m_s^2 - ic \frac{T}{\chi}}, \quad (62)$$

where we have reintroduced the spinon velocity v_s previously set equal to 1. From Eq. (59) we can immediately read off the inverse scattering time Γ for the electron: $\Gamma = -\operatorname{Im} \Sigma$.

D. Fermi surface and electron resonance

We now make the following assumption.

Assumption FS. The neglected short-range attraction between spinon and holon renormalizes the real part of Σ exactly to 0, so that the electron exhibits a Fermi surface.

If assumption FS holds, one might conjecture that this is due to a mechanism somewhat analogous to the one which renormalizes to zero the mass of the two-fermion bound state ("pion") of massless QED_3, whose constituent fermions are dynamically massive.[68] This cancellation between mass and self-energy attractions is there triggered by a symmetry principle, whose analog in our scheme would require further investigation. One should remark that our treatment of the problem resembles the one discussed in Ref. 23 in the $SU(2) \times U(1)$ slave boson approach and in fact it yields a similar structure for the FS, although the scattering time is rather different.

Under assumption FS, finally, for $\vec{q} = \vec{0}$ and $\omega > 0$ small we find the structure (8) with the replacement $Z \to S(\eta) Z$.

This structure shows that the gauge fluctuations are able to bind together spinon and holon into a resonance for low energies and momenta close to the Fermi momenta, but with a wave function renormalization constant which depends both on the point of the FS, due to $S(\eta)$, and the temperature. In particular $Z \sim T^{1/6}$, so Z vanishes if formally extrapolated to $T = 0$. This implies a peculiar non-Fermi-liquid character for this system of "electron resonances." However, a real extrapolation to $T = 0$ cannot be done because the $|\vec{x}|$ saddle point is only dominant for $T \gtrsim \chi m_s Q_0$. The system therefore appears to fit naturally within the scheme of unstable fixed points (UFP's) outlined by Anderson.[69] There it is argued that in general in the renormalization group (RG) formalism, starting at high temperature and energy and integrating out high frequencies one derives a low-temperature and low-frequency model. However, the system does not always flow smoothly under the RG to $T = 0$. It might develop a tendency to approach at intermediate temperatures an infrared UFP. The composite holon-spinon system discussed above yielding the "electron resonance" might be a UFP in the temperature range of validity of our approximations. The angular dependence of the wave-function renormalization $S(\eta)$ yields a reduction of the spectral weight outside the reduced Brillouin zone, in qualitative agreement with ARPES experiments in underdoped cuprates [see Ref. 23 for a similar situation in the $SU(2) \times U(1)$ slave boson approach]. In fact, the intensity measured in ARPES experiments is proportional to $\operatorname{Im} G(\omega, \vec{k}) n(\omega)$; denoting by $I(\vec{k})$ the integrated intensity along the "electron FS" we have a contribution to I due to the "electron resonance" given by

$$I(\vec{n}(\theta) k_F) \sim S(\theta) Z.$$

The factor $S(\theta)$ is peaked around $\theta = 5\pi/4$ [for the FS near $(\pi/2,\pi/2)$] and it is substantially reduced on the opposite side (see Fig. 3).

One might try to extend the analysis performed above for momenta $\vec{q}$ around the holon FS in a shell of thickness Λ, by including the contributions of momenta $\vec{q}$ outside the shell, but still smaller than the UV cutoff of the continuum model. If in this contribution one tentatively neglects the effect of gauge fluctuations which give rise to incoherent component to the "electron" Green function, the essential features of our present consideration will remain; a detailed analysis is in progress.

VI. COMPARISON WITH EXPERIMENTS

A. MIC of in-plane resistivity

Let us now summarize the main results of Sec. IV, useful to derive a formula for the in-plane resistivity ρ, for comparison with the experimental data.

We have shown that (under the stated approximations) the gauge fluctuations exhibit a typical scale, a sort of anomalous skin penetration depth, $Q_0^{-1} \sim \delta^{-2/3} T^{-1/3}$. In the range of temperature identified by $m_s^2 \gtrsim T/\chi \gtrsim m_s Q_0$ the gauge field couples a spinon-antispinon pair into a magnon resonance on a scale triggered by Q_0^{-1}. The resonance exhibits a complex mass term M of "relativistic" structure:

$$M = 2\sqrt{m_s^2 - ic\frac{T}{\chi}}, \tag{63}$$

where $c \sim 3.3$, whose imaginary part appears as a consequence of the dissipative nature of gauge fluctuations for energies smaller than T.

The residue of the complex pole in the magnon resonance correlator is also T dependent and behaves like $Q_0^{-1}(M\kappa)^{1/2}$, where κ is the Landau damping. Using $\vec{j}^s \sim \partial\vec{\Omega} \sim Q_0\vec{\Omega}$ and the Kubo formula for spinon conductivity one obtains

$$\rho_s \sim \frac{m_s^{1/2}}{\sqrt{\delta}} \frac{\left[1 + \left(\frac{\xi}{\lambda_T}\right)^4\right]^{1/8}}{\sin\left[\frac{1}{4}\arctan\left(\frac{\xi}{\lambda_T}\right)^2\right]}, \tag{64}$$

where $\xi \sim |\delta \ln \delta|^{-1/2}$, $\lambda_T \sim (\chi/Tc)^{1/2}$.

For the holons one can borrow a computation performed diagrammatically in Ref. 22 for a Fermi liquid interacting with a gauge field exhibiting a Reizer singularity. Adding, via the Matthiessen rule, the contribution of impurities one finds

$$\rho_h \sim \delta\left[(\epsilon_F \tau_{imp})^{-1} + \left(\frac{T}{\epsilon_F}\right)^{4/3}\right]. \tag{65}$$

For small $\delta, T/t$ we have $\rho_s \gg \rho_h$, so the spinon contribution dominates the physical resistivity in the Ioffe-Larkin rule. For low T, $\rho_s \sim 1/T$, thus exhibiting an insulating behavior, for $T \gtrsim \chi m_s^2$ one finds $\rho_s \sim T^{1/4}$, thus showing a metallic behavior. From formula (64) a MIC is thus recovered

decreasing the temperature, as shown in the experiments discussed in Sec. I C. This crossover is determined by the interplay between the AF correlation length ξ and the thermal de Broglie wavelength λ_T.[70] When $\lambda_T \lesssim \xi$ the "peculiar" localization due to SRAFO is not felt and a metallic behavior is observed. In the opposite limit $\lambda_T \gtrsim \xi$ we find the insulating behavior (but due to the gauge interaction, $\rho_s \neq e^{(\Delta/T)^\alpha}$, a behavior found for a "standard" localization). The doping dependence is rather weak, due to a delicate cancellation in the doping dependence of the dimensionless variable

$$y = \left(\frac{\xi}{\lambda_T}\right)^2 = \frac{Tc}{\chi m_s^2} \sim \frac{Tc}{t|\ln\delta|}, \tag{66}$$

which controls ρ_s; see Eq. (64). Our formula for ρ_s has essentially no free parameters except for an overall resistivity scale. The only parameter $O(1)$ used in our numerical calculations is the coefficient r in the parametrization

$$\chi m_s^2 \sim \frac{t}{6\pi\delta}|\delta \ln \delta| r,$$

which one can fine-tune by using, e.g., the minimum of resistivity for some fixed doping. The entire set of curves $\rho(\delta, T)$ is then completely determined. As shown in Fig. 1 of Ref. 48, the agreement with experimental data is really good, and the MIC temperature goes down, as the doping increasing. If there were no logarithmic correction in our derived spinon mass, there would be no doping dependence *at all* for the MIC temperature.

B. Universal normalized resistivity

Now we consider a more subtle prediction following from our theoretical treatment.

As mentioned in Sec. III A, an inflection point T^* has been observed in heavily underdoped cuprates at a higher temperature, where $d\rho/dT$ has a maximum. Such an inflection point can be tentatively identified with the pseudogap temperature. Such an inflection point also appears in our derived in-plane resistivity formula (we still denote it by T^*), and the "relativistic" structure of the mass term is responsible for it. We find that T^* corresponds to $y \sim 3.4$. Moreover, there is another inflection point in experimental data at low temperatures below which the resistivity exhibits an approximate logarithmic temperature dependence.[41] We propose to identify these two inflection points as the upper and lower bounds for the validity of our approximation and to approximately identify the δ-T parameter region corresponding to the "pseudogap phase" of cuprates. Above the upper inflection point, the system enters the "strange metal" phase to which a separate paper is devoted.[58] Below the lower inflection point, the system also crosses over to a new phase whose properties have to be explored.

Neglecting the $T^{4/3}$ contribution, as justified at low T, from our formula (64) we notice that if we define the "normalized resistivity"
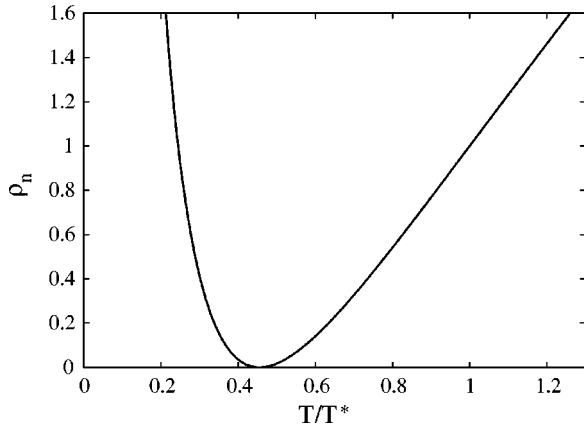
FIG. 4. Calculated "normalized" resistivity ρ_n vs reduced temperature $T/T*$ (see text for explanation).

$$\rho_n(T) = \frac{\rho(T) - \rho(T_{MIC})}{\rho(T*) - \rho(T_{MIC})}, \qquad (67)$$

this is a universal (i.e., doping-independent) function of the variable y, Eq. (66), where T_{MIC} denotes the minimum of ρ_s and one finds it corresponding to $y \sim 1.7$.

This curve has been noticed in the YBCO (Ref. 35) data and quantitatively similar "universal curves" have been observed also for LSCO,[29] BSLCO, and BSCO.[71] (In these last references a different definition of $T*$ was used, based on deviation from linearity of ρ, not directly accessible to our approach and therefore not permitting a direct comparison with our formula. A rough estimate, however, gives for that $T*$ a value dependent on the material, but approximately twice our definition of $T*$.) Our formalism, on the other hand, explains in a neat way their universality character. In Fig. 4 we plot the calculated normalized resistivity ρ_n to be compared with the corresponding experimental curve on LSCO and YBCO that we extracted from the data of Takagi et al.[5] and Trappeniers et al.[35]; see Fig. 5. We did not make any attempts to reconcile the calculated and observed location of the MIC temperature which may depend on factors not included in our consideration but the universal character
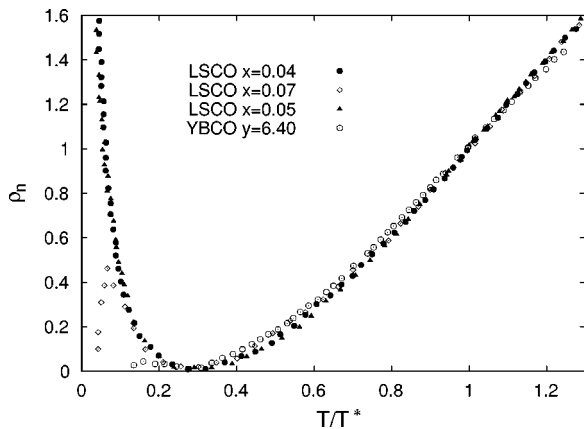

FIG. 5. Temperature dependence for ρ_n in underdoped LSCO (extracted from Ref. 5) and YBCO (extracted from Ref. 35).

of the normalized resistivity is an explicit prediction of theory in agreement with experiment.

Also, the recently experimentally observed a-b asymmetry in the conductivity of LSCO at low temperatures[72,73] has a natural explanation in our framework as due to the anisotropy of the MIC temperature in a-b directions. A detailed explanation will be given in a separate communication.[75]

C. Out-of-plane resistivity

Let us summarize the results of Sec. V needed to compute ρ_c. In the temperature range $m_s^2 \lesssim T/\chi \lesssim m_s Q_0$, the gauge fluctuations couple spinon and holon close to the FS into an "electron" resonance with scattering rate Γ proportional to the inverse lifetime of the magnon; hence

$$\Gamma = -\operatorname{Im} \sqrt{m_s^2 - ic\frac{T}{\chi}} \sim \begin{cases} \dfrac{JT}{t}\left(\dfrac{\delta}{|\ln \delta|}\right)^{1/2}, & \dfrac{T}{\chi m_s^2} \ll 1, \\[12pt] J\left(\dfrac{T\delta}{t}\right)^{1/2}, & \dfrac{T}{\chi m_s^2} \sim 1. \end{cases}$$

$$(68)$$

The wave-function renormalization is the product of a term $S(\theta)$, varying along the FS, where θ is the angle labeling the direction from the center, inherited from the Dirac structure of the holon action, and a T-dependent term Z. This in turn is a product of a term proportional to the "magnon" renormalization constant Z_Ω and a term coming from integration over fluctuations of holons, Gaussian for those along and linear for those perpendicular to the FS, with a scale set by gauge fluctuations, hence giving a contribution $\sim Q_0^{3/2}$:

$$Z \sim Z_\Omega Q_0^{3/2} \sim \sqrt{\delta m_s Q_0}. \qquad (69)$$

To compute ρ_c we average the angular dependence of $S(\theta)$ and insert Eqs. (68) and (69) in KJ's formula, Eq. (10).

It follows from Eqs. (10) and (68) that for low T, $\rho_c \sim T^{-1}$, and for higher temperature, if the first term in Eq. (10) still dominates, $\rho_c \sim T^{-1/2}$ with a coefficient independent of t_c. These features reproduce qualitatively the behavior observed experimentally in several materials (LSCO, YBCO, etc.) in the "pseudogap phase" including the rounded knee cited in Sec. III B, which corresponds to the above change of temperature dependence.

As a consequence of KJ's approach ρ_c at low T appears to give a direct test for the scattering rate of the "electron" in the pseudogap phase. The "metallic" contribution of the second term is important only at higher temperature, where it scales as $T^{1/6}$, causing a further flattening of the $\rho_c(T)$ curves or possibly a minimum. Apart from an overall scale, having already fixed with ρ_{ab} the variable χm_s^2, our formula has only one free parameter, the scale of Z—i.e., essentially the scale λ controlling the cutoff on momenta perpendicular to the FS, $\Lambda = k_F/\lambda$ and weighting the "metallic" contribution. This parameter should be a somewhat large number and might be roughly estimated by fitting ρ_c for one doping concentration. For other dopings the T-dependence behavior of
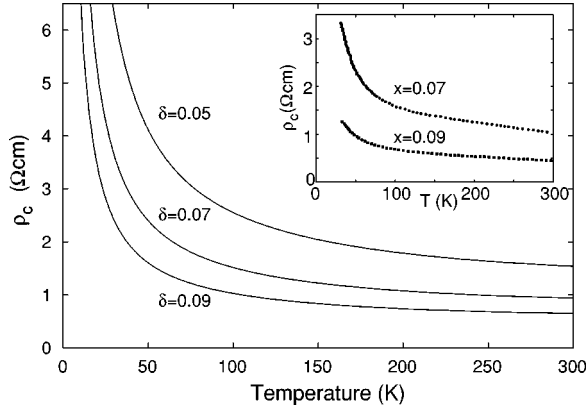
FIG. 6. Calculated temperature dependence of the out-of-plane resistivity (in arbitrary units) for different doping concentrations: $\delta=0.05$ (solid line), $\delta=0.07$ (dashed line), and $\delta=0.09$ (dotted line). Inset shows experimental data on LSCO, extracted from Ref. 77.
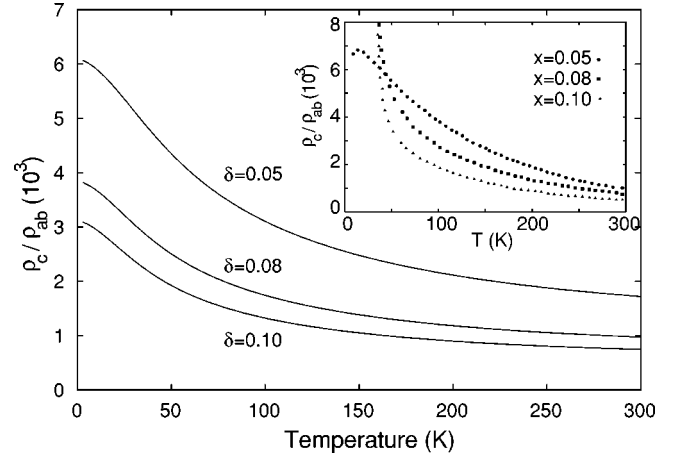

FIG. 7. Calculated temperature dependence of the resistivity anisotropy ratio as a function of temperature for different doping concentrations: $\delta=0.05$ (solid line), $\delta=0.07$ (dashed line), and $\delta=0.09$ (dotted line). Inset shows corresponding experimental data on LSCO, extracted from Ref. 60.

ρ_c is then derived and as one can see from Fig. 6, the theoretical results are in good agreement with experimental data.[59]

Having an explicit theoretical dependence on δ and T for both ρ_c and ρ_{ab} one can further analyze the anisotropy ratio ρ_c/ρ_{ab}. The derived temperature dependence of this ratio is shown in Fig. 7; this ratio clearly saturates at low T, since both ρ_c and ρ scale as $1/T$, but at higher temperature, in the "metallic" region for in-plane resistivity, the ratio decreases like $T^{-1/4}$. Again this behavior is qualitatively consistent with the experimental data in the "pseudogap phase,"[18,41] as shown in the inset of the same figure.

D. Hidden MIC in superconducting cuprates and magnetoresistance

The techniques developed in previous sections are useful to compute other observables, like the transverse in-plane magnetoresistance and the ^{63}Cu spin-lattice relaxation rate. The calculation of magnetoresistance is outlined in Ref. 49; therefore here we only briefly review the results.

The basic underlying hypothesis is that suppressing superconductivity by applying a magnetic field, in superconducting underdoped samples one recovers the normal-state "pseudogap phase."

A magnetic field H perpendicular to the plane then modifies the gauge effective action in two ways: (1) Via a minimal coupling it induces a shift $A\to A-\varepsilon A_{em}$ in the spinon term and $A\to A+(1-\varepsilon)A_{em}$ in the holon term, where ε is the spinon effective charge and A_{em} is the vector potential corresponding to the applied uniform static magnetic field H. In a mean-field treatment the effective charge should be chosen as to satisfy the Ioffe-Larkin rule for diamagnetic susceptibility (see Refs. 49 and 74). Therefore $\varepsilon\sim\chi_h/\chi$. (2) The presence of H induces a parity-breaking Chern-Simons term in the holon action $[\sigma_h(H)/2\pi]A^0\epsilon_{ij}\partial^i A^j$, where $\sigma_h(H)$ is the holon Hall conductivity. Since A_0 is short ranged, with a gap $\gamma=\nu+\omega_p$ [see Eq. (22)], it can be integrated out first, yielding an effective renormalization of the diamagnetic

susceptibility in the transverse action: $\chi\to\chi(H)=\chi+\sigma_h^2(H)/4\pi^2\gamma$ as discussed in Ref. 74. This effect is, however, subleading at low T.

Under the approximations of Sec. IV the result of effects (1) and (2) can be summarized by a modification of the "relativistic" mass term of spinon:

$$M\to M(H)=\sqrt{m_s^2-i\left(\frac{cT}{\chi(H)}-\frac{\varepsilon^2 H^2}{3Q_0^2}\right)}. \qquad (70)$$

(A technical comment: the minimal coupling in the FSF path representation of $G(x,0|F)$ produces a term $\exp\{i\varepsilon\int_0^1 d\lambda\lambda\int_0^s ds'\int_0^{s'} ds''[\phi^i(s')-2p^i][\phi^j(s'')-2p^j]\epsilon_{ij}H\}$ [see Eq. (20)] and evaluating the ϕ integral in Gaussian approximation this term yields a contribution $e^{is^3|\vec{p}|^2 H^2}$ to the Ω correlator in Eq. (31). This finally is responsible for the shift of the last term in the square root in Eq. (70)). The limits of validity of the $|\vec{x}|$ saddle point become $\chi(H)Q_0|M(H)|\lesssim T$, $\text{Im}[M(H)]\lesssim m_s^2$, which for the range of physical parameters considered here ($H\lesssim 100$ T) gives a temperature range still lying between a few tens and a few hundreds degrees. Hence, to conclude, the presence of H modifies ρ_s via the cyclotron effect, by reducing the damping from T/χ to $T/\chi(H)-H^2\varepsilon^2/3Q_0^2$.

This reduction makes the thermal de Broglie wavelength λ_T longer, so the MIC occurs at a higher temperature with respect to the system at $H=0$. The external magnetic field then reveals the MIC originally hidden in the superconducting samples.

Furthermore, the shift of the minimum of ρ causes a strong positive transverse magnetoresistance (MR) at low T, as in fact experimentally seen,[76,77] an effect missing in previous theoretical treatments.[74] At higher temperatures, in the region where dissipation dominates, the shift of diamagnetic susceptibility due to the Chern-Simons term induces a reduction of resistivity, a tendency contrasted by the classical cy-

clotron effect on holons, taken into account in the Boltzmann equation approximation. One then has two possible types of MR curves: one is always positive but it exhibits a knee below the crossover temperature between the mass gap and the dissipation dominated regions (see Fig. 3 in Ref. 49). This behavior can be compared with the one observed in LSCO reported in Ref. 76 and one finds a reasonably good agreement. If, in contrast, the quantum effects related to $\sigma_h(H)$ are sufficiently strong, a minimum develops, eventually leading to a negative MR in some region around it. The MR scales quadratically with H (see Fig. 2 in Ref. 49) in agreement, in particular, with data on LSCO,[77] away from the doping $\delta = 1/8$ where the stripe effects dominate. (In the explicit formula one should also take into account the modification induced by H in the contribution of the Landau damping to Z_j: $\sqrt{\kappa} \to \{[T/\chi(H)]Q_0^{-3} - c'H^2 Q_0^{-5}\}^{1/2}$ where c' is a new constant $\sim f''(Ce^{i\pi/4})$ in fact roughly estimated, together with a parameter coefficient of H in $\sigma(H)$, by comparison with an experimental curve at some doping.)

Finally we notice that in Zn-doped superconducting samples of BSLCO the MIC become observable upon increase of Zn doping (when a magnetic field suppresses superconductivity) and it shifts to higher temperature as the level of Zn doping increases.[45] This effect is qualitatively consistent with our picture. In fact, the Zn doping disturbs the AF background, so making the AF correlation length shorter, therefore shifting the MIC temperature up, although we are not able, at the moment, to make a quantitative estimate of this shift.

E. Spin-lattice relaxation rate

We turn now to the spin-lattice relaxation rate for the Cu sites $(1/T_1)$ (Ref. 63); see Ref. 48. This can be theoretically computed using the Kubo formula

$$\frac{1}{T_1 T} = \lim_{\omega \to 0} \int d^2 q |\vec{A}(\vec{q})|^2 \frac{\mathrm{Im}\,\chi_s(\vec{q},\omega)}{\omega}, \qquad (71)$$

where $\vec{A}(\vec{q})$ is the hyperfine field and $\chi_s(\vec{q},\omega)$ the spin susceptibility. For the Cu sites the hyperfine field $\vec{A}(\vec{q})$ is peaked around $Q_{AF} = (\pi,\pi)$, thus probing the AF spin fluctuations. The electron spin field $\vec{S}(x) = c^\dagger (\vec{\sigma}/2)c(x)$ is related to the spinon and holon fields by

$$\vec{S}(x) \sim [1 - H^* H(x)]e^{i\vec{Q}_{AF}\cdot\vec{x}}\vec{\Omega}(x).$$

Approximating $H^* H$ by its mean field value δ and using the Lehmann representation one finds, for small $\vec{q}$,

$$\lim_{\omega \to 0} \frac{\mathrm{Im}\,\chi_s(\mathcal{Q}_{AF}+\vec{q},\omega)}{\omega}$$

$$\sim \mathrm{Im} \int_0^\infty dx_0 \; ix_0 \int d^2 x (1-\delta)^2 \langle\vec{\Omega}(x)\cdot\vec{\Omega}(0)\rangle e^{i\vec{q}\cdot\vec{x}}.$$

$$(72)$$

The $|\vec{x}|$ and x^0 integrations are performed as in Sec. IV C. Assuming a cutoff for the $|\vec{q}|$ integration in Eq. (71) given by the inverse anomalous skin depth Q_0 and using the smoothness of $\vec{A}(\vec{q})$ at this scale we derive

$$\int d\theta \int_{|\vec{q}|<Q_0} d|\vec{q}||\vec{q}| \quad |\vec{A}(\vec{q})|^2 e^{i\vec{q}\cdot|\vec{x}|(0)\cos\theta} \sim Q_0^2 J_0(Ce^{i\pi/4}).$$

$$(73)$$

Numerically one finds $\mathrm{Re}\,J_0(ce^{i\pi/4}) \equiv a$ and $\mathrm{Im}\,J_0(ce^{i\pi/4}) \equiv b$ with $a/b \sim 0.1$. Plugging Eqs. (73) and (40) into Eq. (72) one obtains, from the Kubo formula (71),

$$(T_1 T)^{-1} \sim (1-\delta)^2 \sqrt{\delta}|M|^{-1/2}$$

$$\times \left[a\cos\left(\frac{\arg M}{2}\right) + b\sin\left(\frac{\arg M}{2}\right) \right]. \quad (74)$$

For low T, $1/T_1 T \sim a + bT$, and for higher T, one finds $1/T_1 T \sim T^{-1/4}$; therefore the spin lattice relaxation rate $(1/T_1 T)$ on Cu sites exhibits a maximum and an inflection point at higher temperature, as observed in YBCO underdoped samples.[78]

If a were 0, then $1/T_1 T$ would be proportional to the spinon conductivity σ_s, and the maximum and inflection point would be at the same temperature of the MIC and T^*, respectively. However, due to the a term in Eq. (74), they are shifted. In particular, the inflection point is found at a lower temperature T_0, in qualitative agreement with the fact that experimentally the pseudogap temperature deduced from the spin-lattice relaxation rate is lower than that derived from the resistivity measurements.[79]

We end this section by remarking that preliminary calculations are giving also encouraging results, when compared with the experimental data, for the electronic ac conductivity at small ω (Ref. 73) and the electronic specific heat (Ref. 80).

VII. CONCLUDING REMARKS

To summarize we have presented in this paper the calculation of physical quantities like the in-plane and out-of-plane resistivities, spin-lattice relaxation rate, etc., within the spin-charge gauge field approach, and compared the theoretical results with experimental data in the pseudogap phase with very good agreement. In particular, we have elucidated the origin of the MIC in the nonsuperconducting cuprates as well as the MIC in superconducting samples when a strong magnetic field suppresses the superconductivity. In our view, this striking phenomenon is an intrinsic property of the pseudogap phase which can shed light on other puzzles in this regime. We are still in the process of studying the diversified properties using our approach in this interesting phase.

There is some skepticism with respect to the gauge field approach in general, mainly because of the strong interactions among the constituent particles. Our attempt in this direction, at least, gives some encouraging signals: if the underlying physics is grasped by the treatment and appropriate nonperturbative tools are employed, there is a fair chance

to correctly describe the puzzling phenomena in the strongly correlated systems. The treatment is not "rigorous" in the mathematical-physics sense, but still acceptable by a "theoretical-physics" standard. Needless to say, the final word belongs to experiments, verifying all consequences of the theoretical interpretation.

The gauge field approach provides us with a nontrivial picture in strongly correlated two-dimensional systems. Unlike the one-dimensional systems where the spin and charge are fully separated and three-dimensional systems where the spin and charge are confined, the spin and charge in two-dimensional systems appear "separated" in their scattering against gauge fluctuations, while being bound into "electron" resonance at a low-energy—momentum scale. In particular, in the "pseudogap phase" the presence of π flux and AF Néel background makes the system "relativistic" with linear dispersion for the holons and spinons "massive" due to interaction with vortices attached to slowly moving renormalized holons. If the system were truly "relativistic," we would have spinon-holon confinement. However, in the actual system the presence of a finite Fermi surface breaks the "bootstrap" symmetry and gives rise to the very peculiar Reizer singularity, producing the spinon-antispinon and spinon-holon binding force. The physical consequences of this nontrivial picture have to be further explored.

[1] T. Timusk and B. Statt, Rep. Prog. Phys. **62**, 61 (1999).

[2] W.W. Warren, Jr. *et al.*, Phys. Rev. Lett. **62**, 1193 (1989); R.E. Walstedt *et al.*, Phys. Rev. B **41**, 9574 (1990); H. Alloul *et al.*, Phys. Rev. Lett. **63**, 1700 (1989); M. Takigawa *et al.*, Phys. Rev. B **43**, 247 (1991).

[3] See, e.g., T. Ito *et al.*, Phys. Rev. Lett. **70**, 3995 (1993); B. Bucher *et al.*, *ibid.* **70**, 2012 (1993).

[4] B. Batlogg *et al.*, Physica (Amsterdam) **235−240**, 130 (1994).

[5] H. Takagi *et al.*, Phys. Rev. Lett. **69**, 2975 (1992).

[6] See, e.g., L.D. Rotter *et al.*, Phys. Rev. Lett. **67**, 2741 (1991); C.C. Homes *et al.*, *ibid.* **71**, 1645 (1993); D.N. Basov *et al.*, *ibid.* **77**, 4090 (1996).

[7] See, e.g., J.W. Loram *et al.*, Phys. Rev. Lett. **71**, 1740 (1993); J.W. Loram *et al.*, Physica (Amsterdam) **282−287**, 1405 (1997).

[8] A.G. Loeser *et al.*, Science **273**, 325 (1996); H. Ding *et al.*, Nature (London) **382**, 51 (1996).

[9] H.J. Tao *et al.*, Physica C **282−287**, 1507 (1997); Ch. Renner *et al.*, Phys. Rev. Lett. **80**, 149 (1998).

[10] M.R. Norman *et al.*, Nature (London) **392**, 157 (1998).

[11] See, e.g., D. Pines, Z. Phys. B: Condens. Matter **103**, 129 (1997) and references therein.

[12] See, e.g., J. Mali, B. Jankó, and K. Levin, Phys. Rev. B **59**, 1354 (1999), and references therein.

[13] Y.J. Uemura *et al.*, Phys. Rev. Lett. **62**, 2317 (1989); M. Randeria *et al.*, *ibid.* **62**, 981 (1989); S. Doniach and M. Inui, Phys. Rev. B **41**, 6668 (1990).

[14] V. Emery and S. Kivelson, Nature (London) **374**, 434 (1995).

[15] L. Balents, M.P.A. Fisher, and C. Nayak, Int. J. Mod. Phys. A **12**, 1033 (1998).

[16] M. Franz and Z. Tesanovic, Phys. Rev. Lett. **87**, 257003 (2001).

[17] See, e.g., M. Randeria, in *Proceedings of the International School "Enrico Fermi" on High Temperature Superconductivity*, edited by G. Iodanisi, J. R. Schrieffer, and M.L. Chiafalo (IOA Press, 1998), pp. 53–75; J.R. Engelbrecht *et al.*, Phys. Rev. B **57**, 13 406 (1998).

[18] P.W. Anderson, Science **235**, 1196 (1987); *The Theory of Superconductivity in the High-Tc Cuprates* (Princeton University Press, Princeton, 1997).

[19] G. Baskaran, Z. Zou, and P.W. Anderson, Solid State Commun. **63**, 973 (1987); G. Kotliar and J. Liu, Phys. Rev. B **38**, 5142 (1988); H. Fukuyama, Suppl. Prog. Theor. Phys. **108**, 287 (1992).

[20] G. Baskaran and P.W. Anderson, Phys. Rev. B **37**, 580 (1988).

[21] L. Ioffe and A. Larkin, Phys. Rev. B **39**, 8988 (1989).

[22] P.A. Lee and N. Nagaosa, Phys. Rev. Lett. **65**, 2450 (1990); Phys. Rev. B **46**, 5621 (1992); L.B. Ioffe and P.B. Wiegmann, Phys. Rev. Lett. **65**, 653 (1990).

[23] X.G. Wen and P.A. Lee, Phys. Rev. Lett. **76**, 503 (1996); P.A. Lee *et al.*, Phys. Rev. B **57**, 6003 (1998).

[24] I. Ichinose *et al.*, Phys. Rev. B **64**, 104516 (2001).

[25] T. Senthill and M.P.A. Fisher, Phys. Rev. B **62**, 7850 (2000); cond-mat/0008082 (unpublished).

[26] S. Sachdev, *Quantum Phase Transitions* (Cambridge University Press, Cambridge, England, 1999).

[27] C. Castellani *et al.*, Z. Phys. B: Condens. Matter **103**, 137 (1997).

[28] J. Zaanen, cond-mat/0103255 (unpublished); S. Chakravarty *et al.*, Phys. Rev. B **63**, 094503 (2001).

[29] J.L. Tallon *et al.*, Status Solidi B **215**, 531 (1999); J.L. Tallon *et al.*, cond-mat/0211048 (unpublished).

[30] K.M. Lang *et al.*, Nature (London) **415**, 412 (2002).

[31] J. Zaanen, Nature (London) **415**, 379 (2002).

[32] J.X. Zhu *et al.*, Phys. Rev. Lett. **87**, 197001 (2001); Q.H. Wang, *ibid.* **88**, 057002 (2002); D.K. Morr, *ibid.* **89**, 106401 (2002).

[33] B. Keimer *et al.*, Phys. Rev. B **46**, 14 034 (1992).

[34] A.T. Fiory *et al.*, Phys. Rev. B **41**, 2627 (1990).

[35] B. Wuyts *et al.*, Phys. Rev. B **53**, 9418 (1996); L. Trappeniers *et al.*, J. Low Temp. Phys. **117**, 681 (1999).

[36] Y. Ando *et al.*, Phys. Rev. Lett. **83**, 2813 (1999).

[37] S. Ono and Y. Ando, Phys. Rev. B **67**, 104512 (2003).

[38] Y. Onose *et al.*, Phys. Rev. Lett. **87**, 217001 (2001).

[39] P. Fournier *et al.*, Phys. Rev. Lett. **81**, 4720 (1998).

[40] Y. Ando *et al.*, Phys. Rev. Lett. **87**, 017001 (2001).

[41] Y. Ando *et al.*, Phys. Rev. Lett. **75**, 4662 (1995); Y. Ando *et al.*, J. Low Temp. Phys. **105**, 867 (1996).

[42] G.S. Boebinger *et al.*, Phys. Rev. Lett. **77**, 5417 (1996).

[43] Y. Ando *et al.*, Phys. Rev. Lett. **77**, 2065 (1996).

[44] S. Ono *et al.*, Phys. Rev. Lett. **85**, 638 (2000).

[45] Y. Fukuzumi *et al.*, Phys. Rev. Lett. **76**, 684 (1996); K. Segawa

and Y. Ando, Phys. Rev. B **59**, P3948 (1999); Y. Hanaki *et al.*, *ibid.* **64**, 172514 (2001).

[46] P.W. Anderson *et al.*, Phys. Rev. Lett. **77**, 4241 (1996); C.M. Varma, *ibid.* **79**, 1535 (1997); A.D. Mirlin and P. Wölfle, Phys. Rev. B **55**, 5141 (1997).

[47] P.A. Marchetti, Z.B. Su, and L. Yu, Phys. Rev. B **58**, 5808 (1998).

[48] P.A. Marchetti, J.H. Dai, Z.B. Su, and L. Yu, J. Phys.: Condens. Matter **12**, L329 (2000).

[49] P.A. Marchetti, Z.B. Su, and L. Yu, Phys. Rev. Lett. **86**, 3831 (2001).

[50] R.T. Birgenau *et al.*, Phys. Rev. B **38**, 6614 (1988).

[51] J. Fröhlich and P.A. Marchetti, Phys. Rev. B **46**, 6535 (1992).

[52] In taking scaling limit we neglect short-range couplings; we assume that they should be taken into account after the treatment of long-range interactions mediated by the gauge field. The additional induced corrections are not discussed in this paper.

[53] J. Fröhlich and U. Studer, Rev. Mod. Phys. **65**, 733 (1993); J. Fröhlich, R. Götschmann, and P.A. Marchetti, J. Phys. A **28**, 1169 (1995).

[54] J. Fröhlich, R. Götschmann, and P.A. Marchetti, Commun. Math. Phys. **173**, 417 (1995).

[55] M. Reizer, Phys. Rev. B **39**, 1602 (1989); **40**, 11 571 (1989).

[56] J. Fröhlich *et al.*, Nucl. Phys. B **374**, 511 (1992).

[57] P.A. Marchetti, Z.B. Su, and L. Yu, Nucl. Phys. **B482**, 731 (1996).

[58] P.A. Marchetti, G. Orso, Z.B. Su, and l. Yu (unpublished).

[59] T. Ito *et al.*, Nature (London) **B350**, 596 (1991); Y.F. Yan *et al.*, Phys. Rev. B **52**, R751 (1995).

[60] S. Komiya *et al.*, Phys. Rev. B **65**, 214535 (2002).

[61] N. Kumar and A.M. Jayannavar, Phys. Rev. B **45**, 5001 (1992); N. Kumar *et al.*, Mod. Phys. Lett. B **11**, 347 (1997); Phys. Rev. B **57**, 13 399 (1998).

[62] H.M. Fried and Y.M. Gabellini, Phys. Rev. D **51**, 890 (1995).

[63] A. Luther, Phys. Rev. B **19**, 320 (1979); F.D.M. Haldane (unpublished).

[64] G. Benfatto and G. Gallavotti, J. Stat. Phys. **59**, 541 (1990); R. Shankar, Rev. Mod. Phys. **66**, 129 (1994).

[65] J. Fröhlich *et al.* (unpublished).

[66] A.V. Svidzinsky, Sov. Phys. JETP **4**, 179 (1957).

[67] L. De Leo, Laurea thesis, University of Padova, 2000.

[68] E. Dagotto, A. Kocic, and J.B. Kogut, Nucl. Phys. B **334**, 279 (1990).

[69] P.W Anderson, Physica B **318**, 28 (2002).

[70] The magnetic correlation length in our approach should not be identified with that appearing in the coefficient of the q^2 term in a representation in the manner of Pines of the spin susceptibility, which turns out to be T dependent. Equation (34) suggests that it could be identified with the correlation length measured by the equal time spin correlator at low T.

[71] Z. Konstantinovic *et al.*, Physica C **341**, 859 (2000).

[72] Y. Ando *et al.*, Phys. Rev. Lett. **88**, 137005 (2002).

[73] M. Dumm, D.N. Basov, S. Komiya, and Y. Ando, Phys. Rev. Lett. **91**, 077004 (2003).

[74] L. Ioffe and G. Kotliar, Phys. Rev. B **42**, 10 348 (1990); L. Ioffe and P. Wiegmann, *ibid.* **45**, 519 (1992).

[75] P.A. Marchetti, G. Orso, Z.B. Su, and L. Yu (unpublished).

[76] A. Lacerda *et al.*, Phys. Rev. B **49**, 9097 (1994).

[77] T. Kimura *et al.*, Phys. Rev. B **53**, 8733 (1996); Y. Abe *et al.*, *ibid.* **59**, 14 753, (1999).

[78] C. Berthier *et al.*, Physica C **235−240**, 67 (1994).

[79] M. Imada, A. Fujimori, and Y. Tokura, Rev. Mod. Phys. **70**, 1039 (1998).

[80] J.W. Loram *et al.*, J. Phys. Chem. Solids **59**, 2091 (1998).